CHAPTER - VI

GEOCHEMISTRY

CHAPTER-VI

GEOCHEMISTRY

After a critical appraisal of petrographic characters and mineral chemistry of the coexisting phases in different lithounits, 42 samples were selected for chemical analyses. Out of these major oxides of 9 samples were determined by routine method, 5 samples by XRF spectrometry. Major oxides of pelitic and calc granulites for 12 samples are by routine method and 2 representative samples by XRF. Trace elements and REE for 6 representative charnockitic rocks (including basic and ultrabasic varieties), 1 sample of Erinpura Granite and 2 samples of pelitic and 1 sample of calc granulite were determined by ICP-MS. Apart from these, the trace elements of 9 smaples were determined by AAS.

MS-1	Charnockite near Balaram
MS-2	Intermediate charnockite, Balaram
MS-3	Basic Charnockite, Chikanwas
MS-4	Basic Charnockite, Kanpura
MS-5	Meta-norite, Ajapur Wanka
MS-6	Ultrabasic Charnockite, Kanpura
MS-7	Pelitic granulite, Diwania hill
MS-9	Erinpura granite
MS-10	Calc granulite
SJMP-1 & 2	Ultrabasic granulites
SJMP-3	Basic Granulite
SJMP-4 & 5	Norite
SJMP-6 & 7	Intermediate Granulite
SJMP-8 & 9	Acid Ganulites (Charnockite)
SJMP-10-21	Pelitic Granulite
SJMP-22	Calc Granulite

VI.1 *Analytical Techniques used*

Major oxides of the various rocks were estimated by X-Ray Fluorescence at NGRI, Hyderabad. Trace elements and Rare Earth Element concentration in the various rocks were determined by Inductively Coupled Plasma - Emission Mass Spectrometry

(ICP-MS) at NGRI, Hyderabad. Concentrations are in microgram/ millilitre. Internal standards used are Rh and Bi in case of Sample Nos. MS-1 through MS-5 (French Standard AC-E, 1994) and in case of MS-6 through MS-10 internal standard is Rh (GSJ standards (Japanese) JG-2, 1994 - granite).

Some of the trace elements viz. Cr, Ni, Zn, Mn, Cu etc were determined by AAS. In case of samples Nos. MAL-1 to MAL-10, the following parameters were used :

Instrument Parameters

System type	Flame	Flame	Flame	Flame	Flame
Element	**Zn**	**Cu**	**Mn**	**Fe**	**Al**
Matrix	Testinstall for all.				
Lamp current	5.0 mA	4.0	5.0	7.0	10.0
Wave length nm	213.9	324.7	279.5	248.3	396.2
Slit width nm	0.5	0.5	0.2	0.2	0.5
Slit height	Normal	Normal	Normal	Normal	Normal
Instrument Mode	BC on	BC off	BC off	BC on	BC off
Absorbance					
Sampling mode	Manual	Manual	Manual	Manual	Manual

Gas Control Parameters

Flame Type	Air-Acetylene	Air-Acetylene	Air-Acetylene	Air-Acetylene	N2O-Acetylene
Acetylene Flow	1.33	1.33	1.33	1.33	5.20
Air flow	10.0	10.0	10.0	10.0	10.0

Flame Sampling Parameters

Recalibration Rate	0	0	0	0	0
Rescale Rate	0	0	0	0	0
Rescale Std. No.	2	2	2	2	2

Data Collection Parameters

Read Time (s)	3.0	3.0	3.0	3.0	3.0
Time Constant (s)	0.0	0.0	0.0	0.0	0.0
Expansion Factor	1	1	1	1	1

Instrument Parameters

System type	Flame	Flame
Element	Ni	Cr
Matrix	Testinstall	
Lamp current mA	5.0	6.0
Wave length nm	232.0	357.9
Slit width nm	0.2	0.2
Slit height	Normal	Normal
Instrument Mode	BC on	BC off
Absorbance		
Sampling mode	Manual	Manual

Gas Control Parameters

Flame Type	Air-Acetylene	N2O-Acetylene
Acetylene Flow	1.33	5.50
Air flow	10.0	10 0

Flame Sampling Parameters

Recalibration Rate	0	0
Rescale Rate	0	0
Rescale Std. No.	2	2

Data Collection Parameters

Read Time (s)	3.0	3.0
Time Constant (s)	0.0	0.0
Expansion Factor	1	1

Analytical data (AAS) values are in micrograms/ml

Sample No.	Rock type	Al	Zn	Cu
1.	Granite BR	61.732	0.637	0.127
2.	Acid Charnockite BRQ	58.43	0.556	0.181
3.	Pelitic granulite SH	58.816	0.443	0.159
4.	Basic Charnockite Mo	72 633	0.478	0.124
5.	Basic Charnockite BQ	75.120	0.481	0.127
6.	Basic Charnockite Ajp W	79.495	0.471	0.168
7.	Ultrabasic charnockite Ajp W	94.15	0.395	0.156
8.	Basic Charnockite Chikanvas Q	78.917	0.333	0 120
9.	Ultrabasic Charnockite Kanpura	44.418	0.343	0.132

Sample No.	Rock type	Mn	Ni	Cr
1.	Granite BR	1.983	0.449	14 269
2.	Acid Charnockite BRQ	0.261	<0.01	<0.01
3.	Pelitic granulite SH	0.19	<0.01	<0.01
4.	Basic Charnockite Mo	0.556	<0.01	0 089
5.	Basic Charnockite BQ	0.507	<0.01	<0.01
6.	Basic Charnockite Ajp W	0.555	<0.01	0.200
7.	Ultrabasic charnockite Ajp W	0.674	<0.01	0.165
8.	Basic Charnockite Chikanvas Q	0.512	<0.01	<0 01
9.	Ultrabasic Charnockite Kanpura	0.551	0.195	0.542

VI.2 PYROXENE GRANULITES

Chemical analyses of various pyroxene granulites viz. ultrabasic Charnockite, basic charnockite, olivine norite, intermediate charnockite and acid charnockite have been plotted on various binary and ternary diagrams to show their chemical behaviour and to derive their possible genesis.

In **Fig 6.1 A-H** various oxides have been plotted against SiO2. With the increasing SiO2, the following trends are observed :

1. TiO2 shows marginal increase with increase in SiO2 in acid and intermediate charnockites **(Fig. 6.1A)**.
2. Al2O3 increases slightly from basic to intermediate charnockites **(Fig. 6.1B)**.
3. FeO* decreases from ultrabasic to acid charnockites **(Fig. 6.1C)**.
4. MgO decreases from ultrabasic to basic charnockites sharply, less so from basic to intermediate charnockites and very slightly from intermediate to acid charnockites **(Fig.6.1D)**
5. CaO decreases from basic to acid charnockites **(Fig.6.1E)**.
6. Both K2O & Na2O increase from ultrabasic to acid varieties. But K2O shows more enrichment in acid types **(Fig. 6.1 F & G)**.
7. No significant trend is seen in P2O5 **(Fig. 6.1 H)**

In the Q-Ab-Or and Ab-An-Or diagrams, it is observed that acid charnockites plot in granite field, intermediate charnockites in the adamellite (MS-2)/ granodiorite (S-6, S-7) field and basic charnockites in the tonalite field **(Fig. 6.2 A & B)**. CaO-Na2O-K2O plots of Charnockite show gradual increase in K2O content from ultrabasic to acid types and are closely similar to those of South India (Condie and Allen, 1984) and Lewisian acid granulite (Rollinson and Windley, 1980a). All the charnockites (except ultrabasic variety) plot within quartz-diorite and granodiorite fields **(Fig. 6.3A)**.

In the AFM diagram, the acid charnockites plot in the calc alkaline field while basic rocks plot in tholeiitic field and correspond to the field of Australian basic granulites (Wilson, 1978). There is distinct iron enrichment trend **(Fig. 6.3B)** which is characteristic of Archaean tholeiite (Lingadevaru et al, 1996).

In the FeO/MgO vs TiO2 plots, the basic charnockites plot in the ridge tholeiite and island arc tholeiite **(Fig. 6.4A)**.

In the Na2O/K2O vs Na2O+K2O diagram, the protoliths of basic charnockites are indicative of protoliths of island arc type (Miyashiro, 1973, Fig. 6.4B).

In the SiO2 vs FeO/MgO diagram, most of the charnockite plots are within tholeiitic field. In the FeO/MgO vs SiO2, TiO2, Al2O3, CaO and MgO

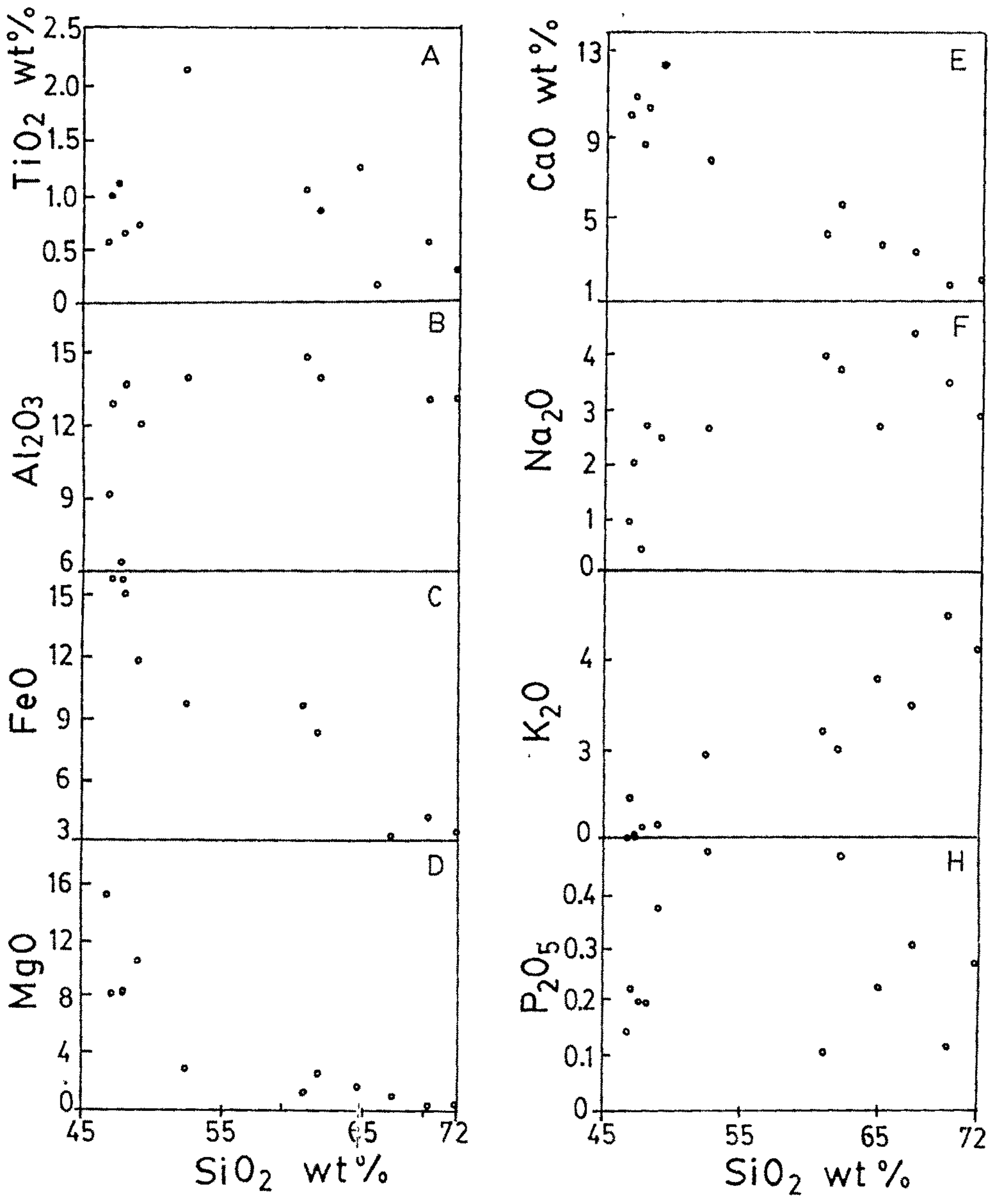

Fig. 6.1 **A-H Plot of various oxides vs SiO2 in 2-pyroxene granulites.**

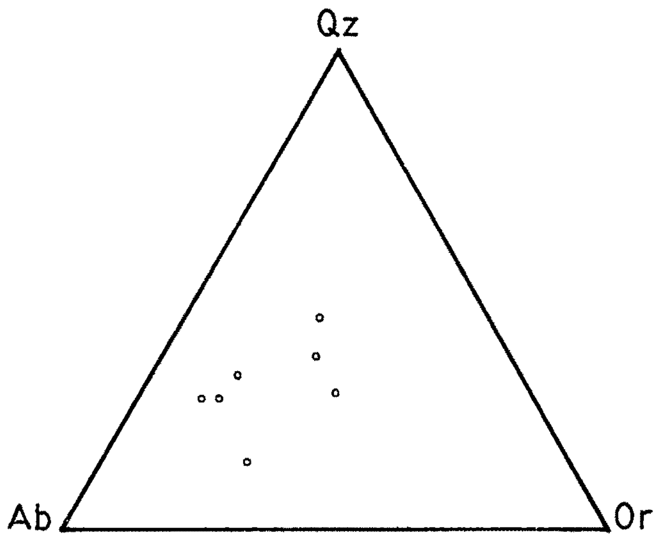

Fig. 6.2A **Q_z-Ab-Or diagram of 2-pyroxene granulites**

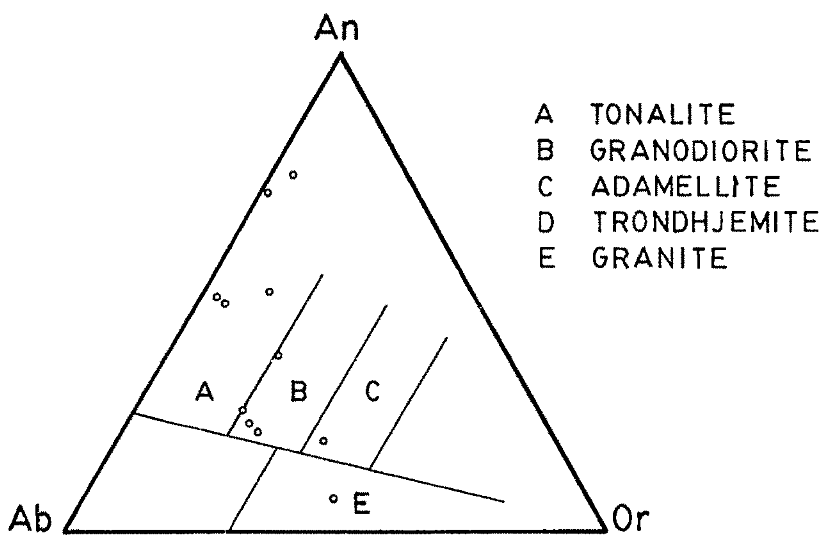

Fig. 6.2B **Ab-An-Or diagram of 2-pyroxene granulites.**

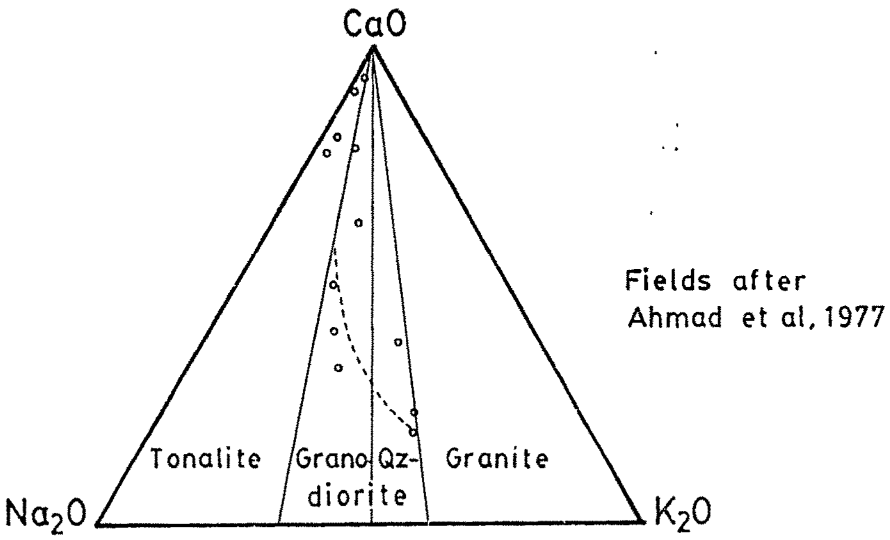

Fig. 6.3A CaO-Na2O-K2O plots of 2-pyroxene granulites.

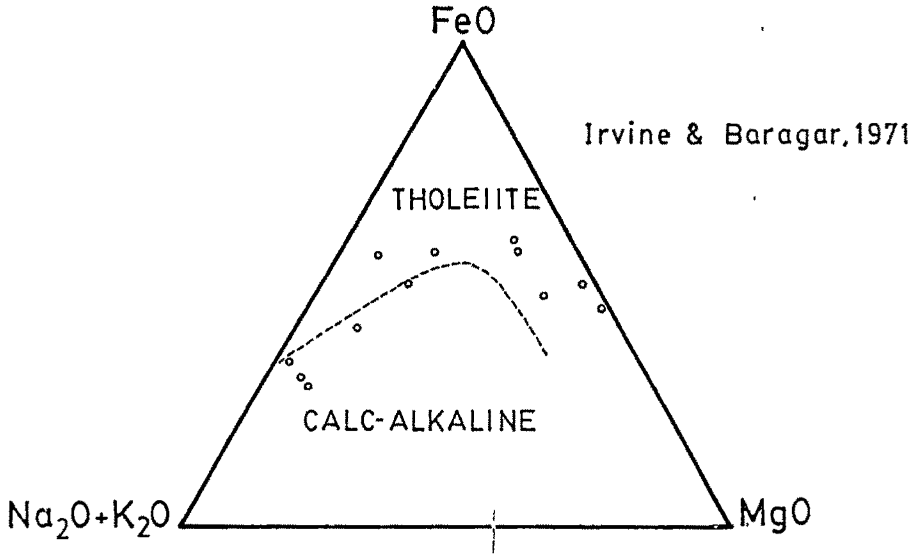

Fig. 6.3B AFM diagram of 2-pyroxene granulites.

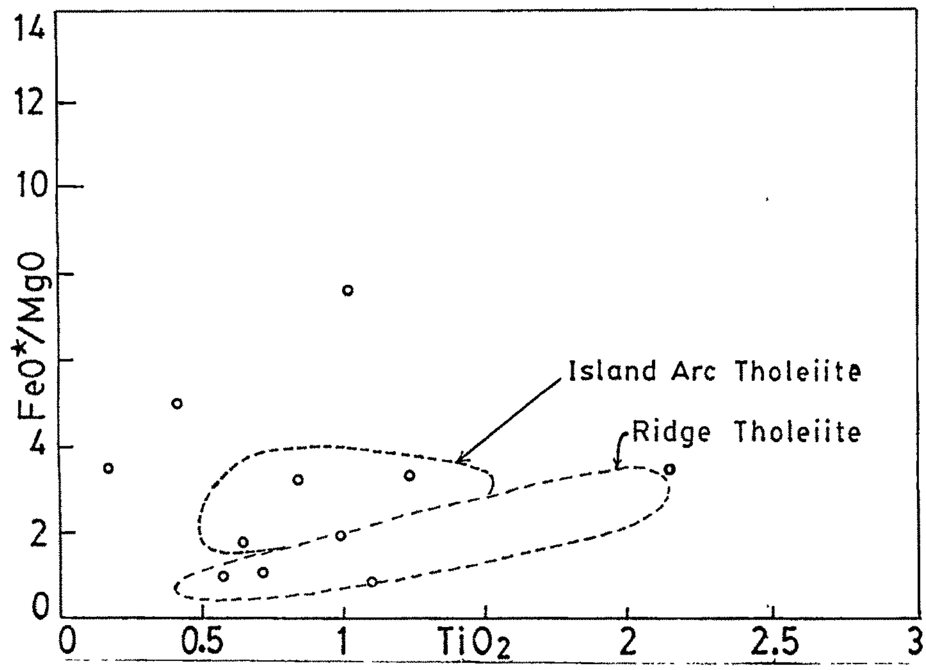

Fig. 6.4A FeO/MgO vs TiO2 plots of 2-pyroxene granulites.

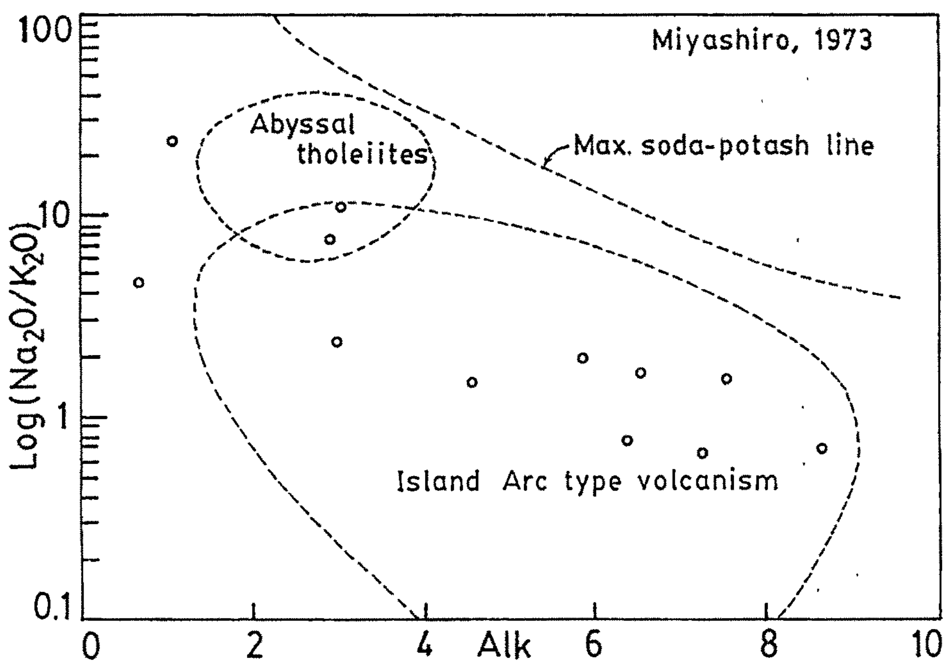

Fig. 6.4B log (Na2O/K2O) vs Alkalies (Na2O+K2O) diagram, the protoliths of basic charnockites (Miyashiro, 1973)

(**Fig. 6.5 A-E**), MgO and CaO are seen to decrease with SiO2 increase.

Trace elements Ni and Zr vs FeO/MgO for the basic charnockites (**Fig. 6.6A and 6.6B**) show that basic granulite is strikingly comparable to those of Central Rajasthan (Gyani & Omar, 1996) and Madras (Chakraborty & Sen , 1983).

In the Zr-Yb-Nb discrimination diagram (Meschede, 1986), some of charnockites plot in E-type MORB (Mid Oceanic Ridge Basalt), Within Plate (WP) tholeiite and VAB (Volcanic Arc Basalt) and N-type MORB (**Fig. 6.7A**). Similar trend is observed in Th-Hf-Ta and Th-Hf-Nb diagrams (Wood, 1980) (**Fig. 6.7 B,C**).

In Zr/y vs Log Zr diagram of Pearce and Norry (1979) (**Fig. 6.8A**) and Th/Yb vs Ta/Yb plots (**Fig. 6.8B**) a comparison of different charnockites from S.India (Pallavaram), Rajasthan (Deogarh-Nashirabad and Bhinai, after Gyani et al, 1996) and N. Gujarat has been attempted.

In the ACF diagram, the basic charnockites are seen to be within the metabasite field of Adirondack region (after De Waard, 1965) and plot in the plagioclase-orthopyroxene-clinopyroxene, indicating products of granulite facies metamorphismc (**Fig. 6.9**). The acid charnockites lie on anorthite-orthopyroxene line of the anorthite-garnet-orthopyroxene field.

Rb-Sr ratio (**Fig. 6.10A**) for acid and intermediate charnockites is >0.2 and is comparable to acid charnockites of Deogarh-Nashirabad, Pallavaram and those from China. For the basic charnockites, Rb/Sr is between 0.1 and 0.2 and. For the ultrabasic charnockite, it is near the mantle value i.e. 0.03. For the norite, it is between 0.02-0.03. With the assimilation of crustal material, the Rb/Sr values in gneiss and acid granulite has increased (>0.2), in other words, acidic magma derived from upper mantle/ lower crust had been contaminated by crustal material prior to granulite facies metamorphism producing acid (quartzo-feldspathic) granulites.

In the K% vs Rb content, acid charnockites plot close to charnockites of Pallavaram and Arcot. In general K/Rb values remain between 250-550, indicative of igneous precursor. The K/Rb (140-398) is comparable to those of igneous rocks (230). K/Rb (<500) is characteristic of rocks of Archaean age. K/Rb is 341 for Madras charnockites which is comparable to Balaram Charnockite (307).

In the K2O - Rb plots, the charnockites show a close similarity with those from Deogarh-Nashirabad (Gyani et al, 1996), the charnockites from South India and the Qianan province of China (**Fig. 6.10B**).

Rb/Sr ratio [1 83 (acid charnockite), 1 45 (intermediate charnockite), 0 028 (norite), 0.136-0.216 (basic charnockites), 0.044 (ultrabasic charnockite)] are congruent to the expected igneous lithologies The Mg Number of the basic granulites is 34.38 which is <45, suggests, low degree of differentiation of primary magma (Lingadevaru et al, 1996).

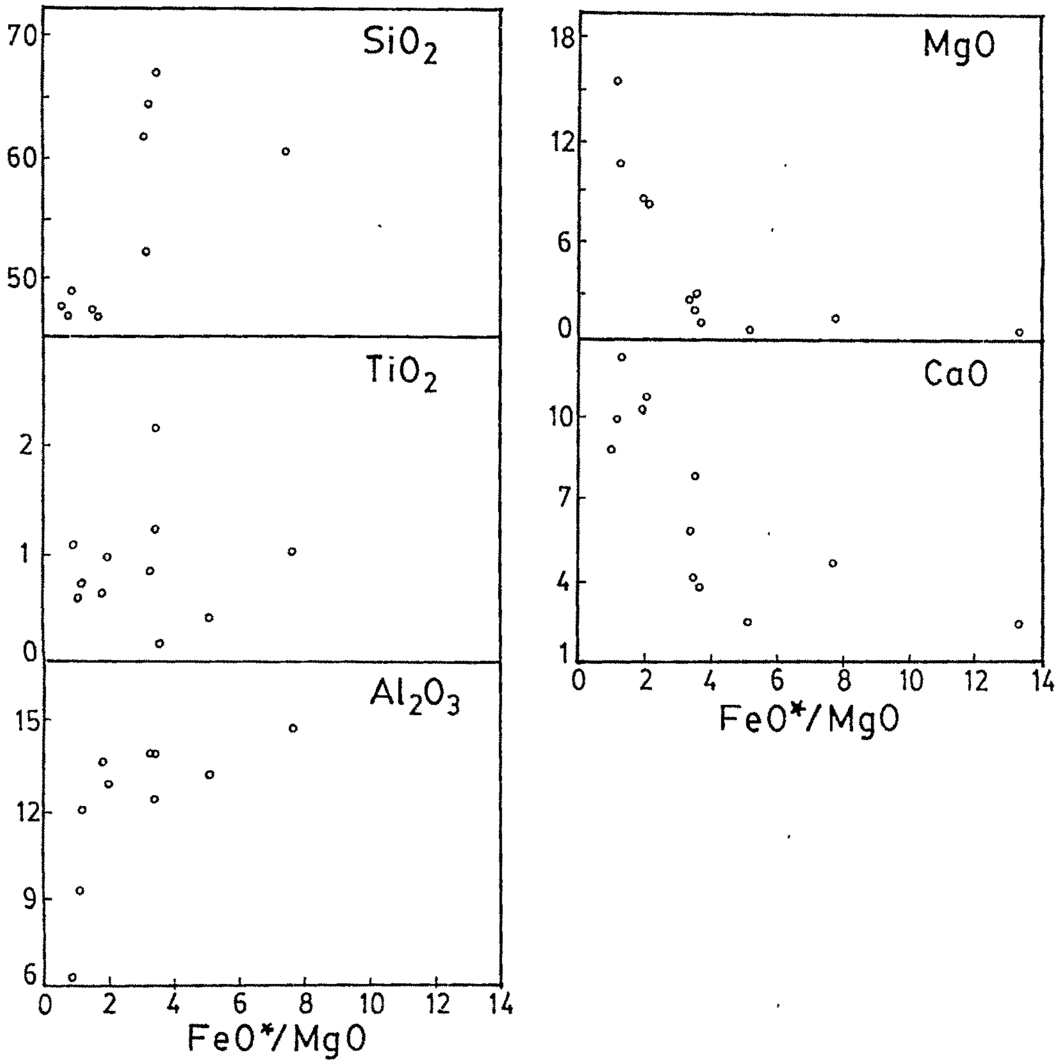

Fig. 6.5 **FeO/MgO vs various oxides in 2-pyroxene granulites.**

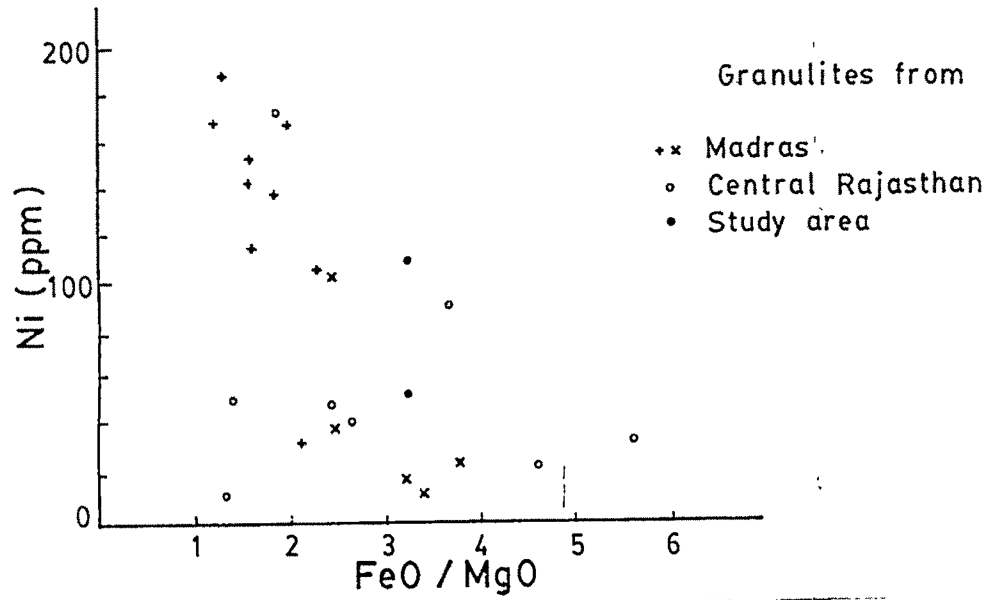

Fig. 6.6A **Ni vs FeO/MgO plots of basic granulites**

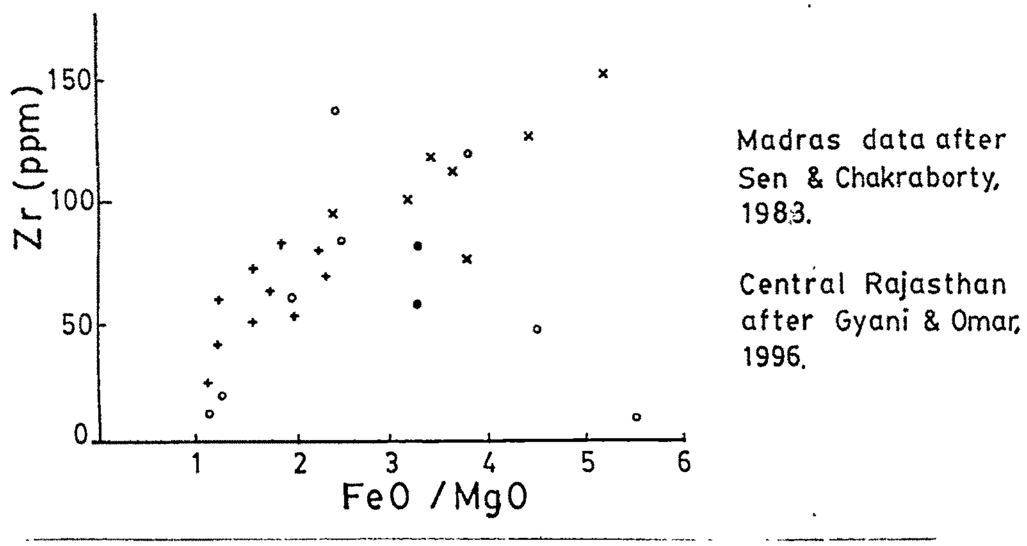

Fig. 6.6B **Zr vs FeO/MgO plots of basic granulites**

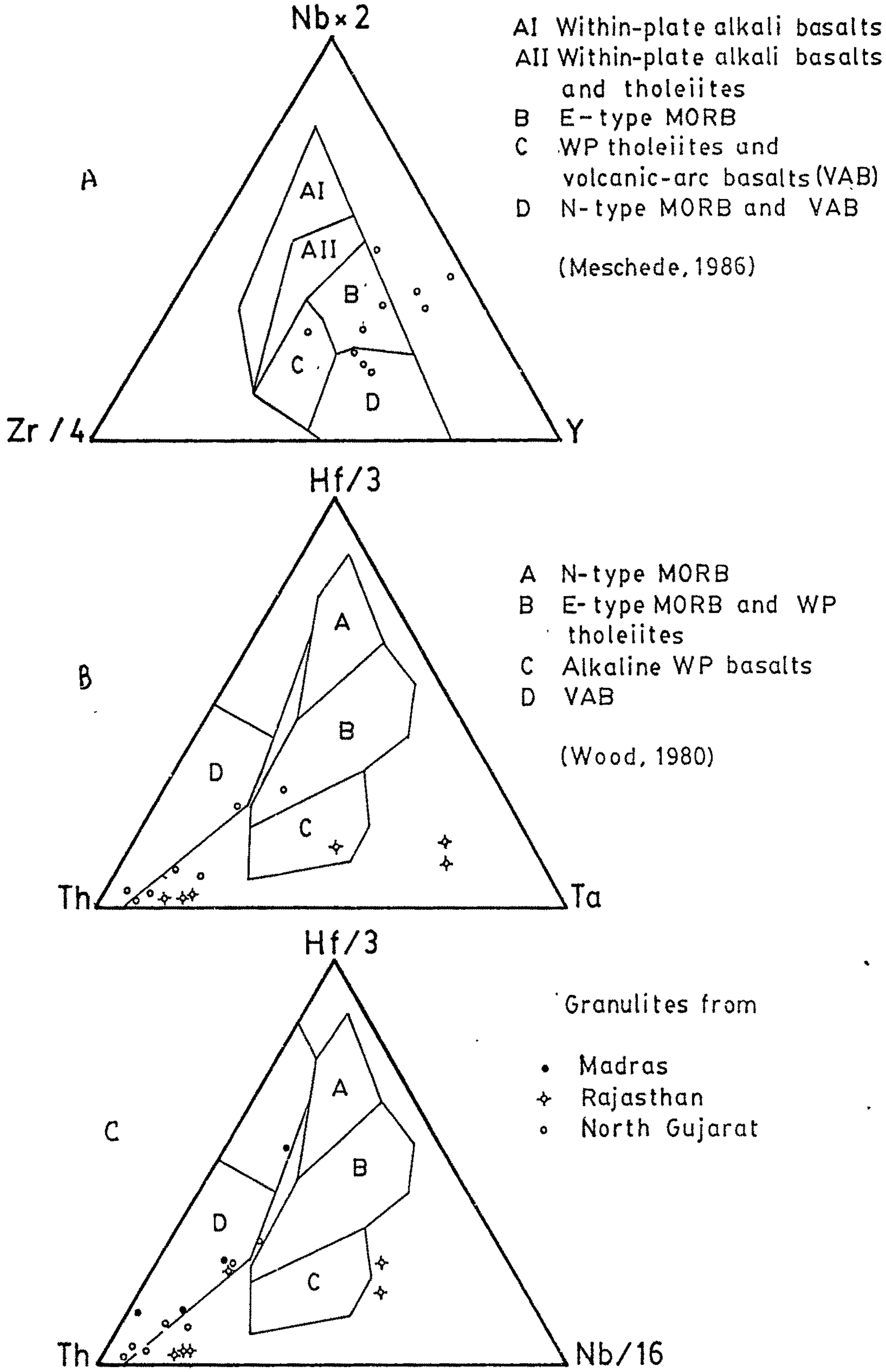

Fig. 6.7A Zr-Yb-Nb discrimination diagram (Meschede, 1986)

Fig. 6.7B Th-Hf-Ta diagram (Wood, 1980)

Fig. 6.7C Th-Hf-Nb diagram (Wood, 1980)

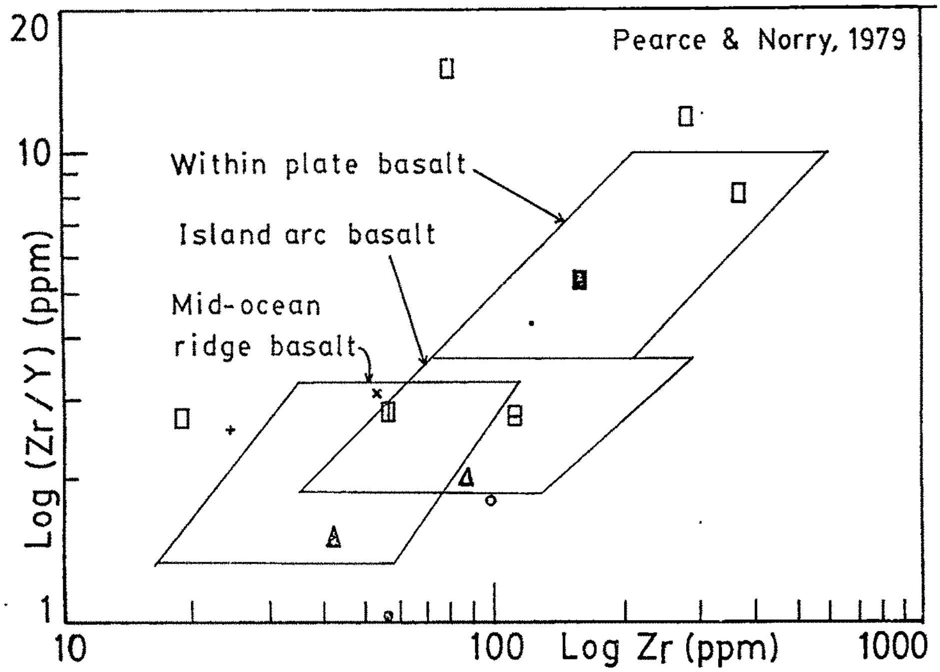

Fig. 6.8A **Log (Zr/Y) vs Log Zr plots after Pearce & Norry (1979)**

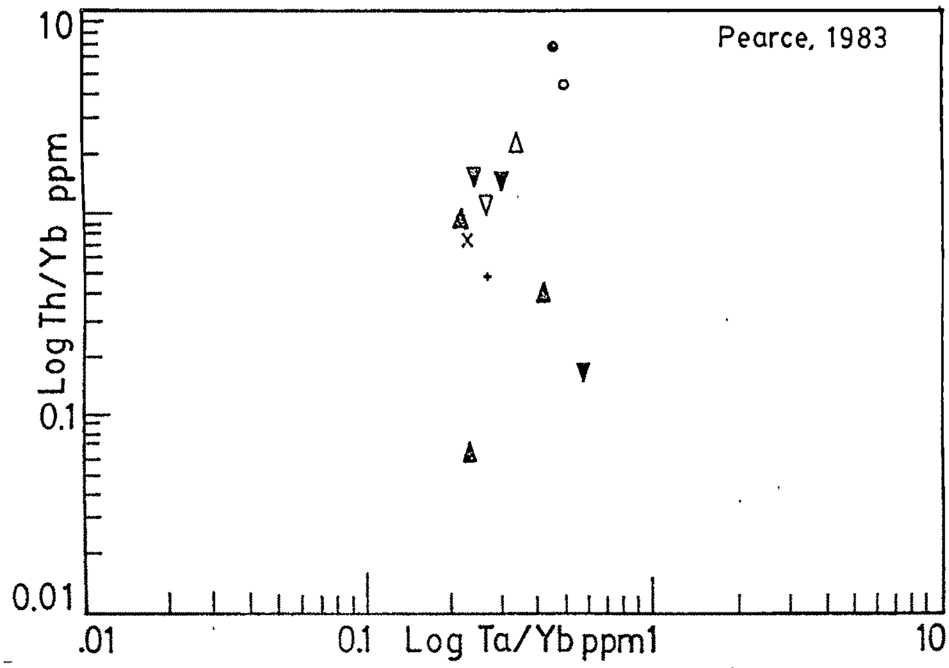

Fig. 6.8B **Log (Th/Yb) vs Log (Ta/Yb) plots showing comparison with other granulites of India.**

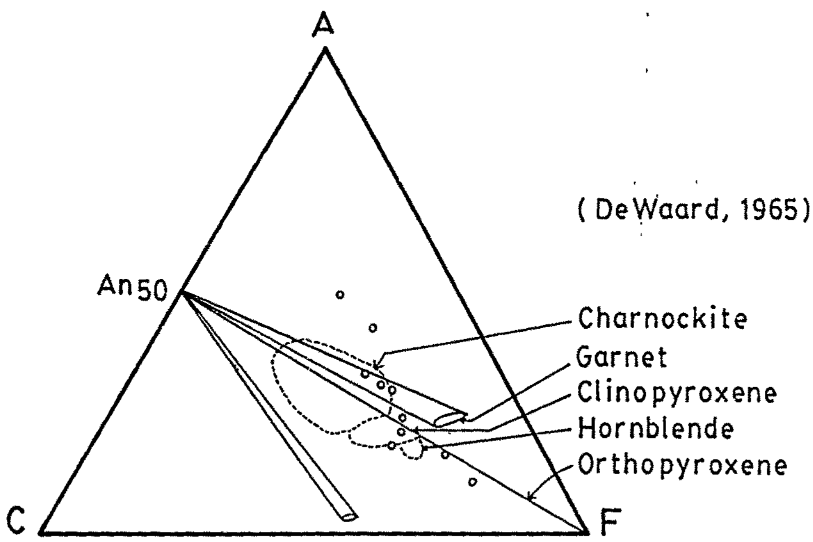

Fig. 6.9 ACF diagram of 2-pyroxene granulites.

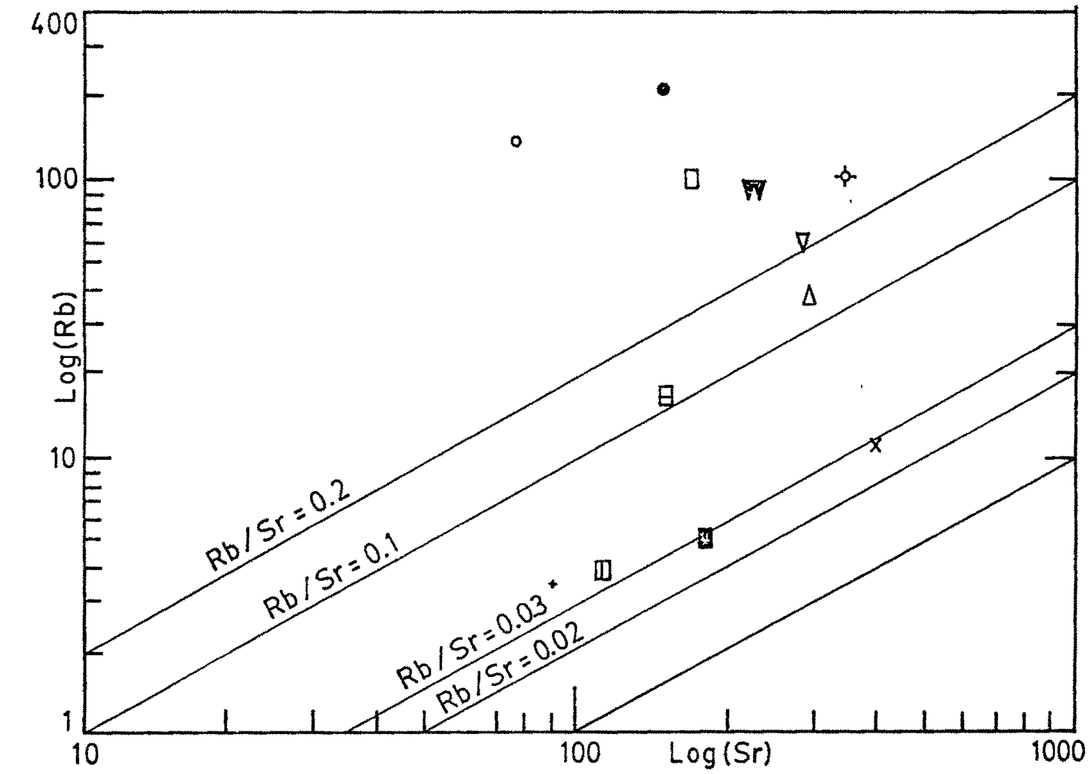

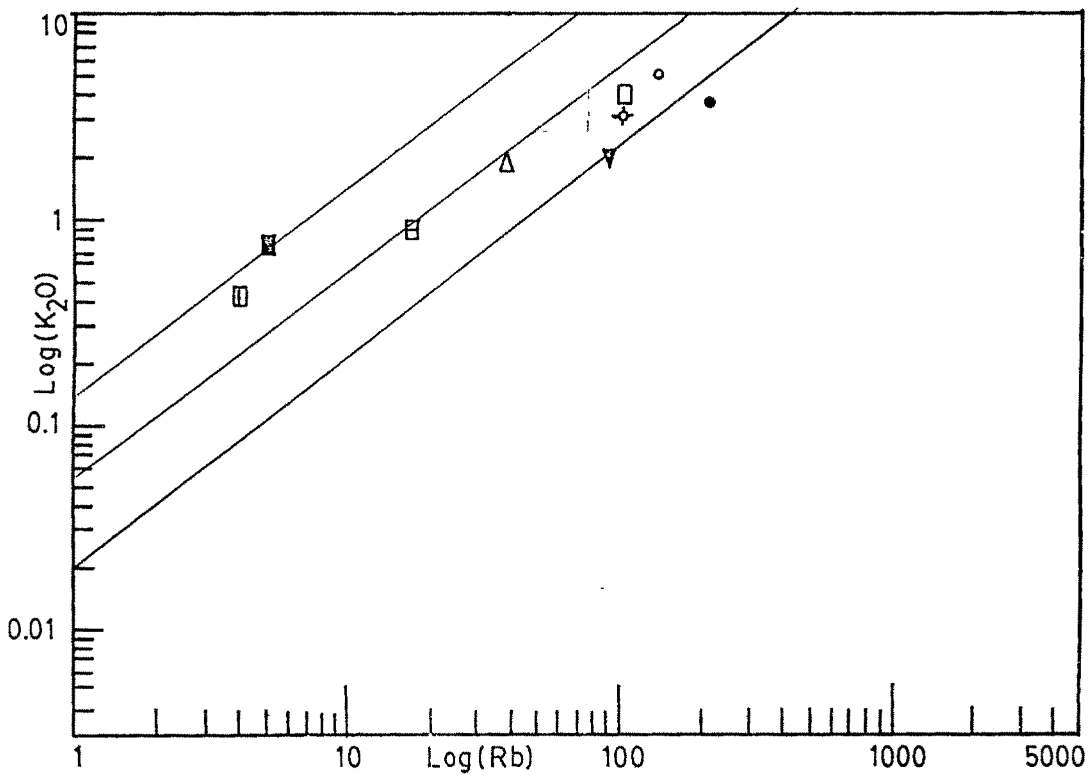

Fig. 6.10A Log Rb - Log Sr plots of 2-pyroxene granulites.

Fig. 6.10B Log K2O - Log Rb plots of 2-pyroxene granulites.

The Rb/Sr ratio of the basic charnockites is of much significance. The plots lie close to the Rb/Sr values of upper mantle (0.01-0.03) which suggests mantle derived magmatic source for the protoliths.

Th has been plotted against Rb, Cs and U **(Fig. 6.11 A,B,C)**. In the Rb-Th plots, the charnockites show Archaean affinity (Allen, 1984). Cs and U decrease with decrease in Th and are comparable to similar rocks from Nilgiri, Shevaroy Hills, Toppur and other rocks of South India (Condie and Allen, 1984).

For acid charnockites ΣREE is 479.74, ΣLREE is 425.77 and ΣHREE 53.97. (La/Lu)N = 11.71; Eu/Sm = 0.158, (Ce/Yb)N = 8.67 and (La/Yb)n = 9.45.

For Basic charnockites ΣREE is 94.17 - 219.88, ΣLREE is from 77.27 to 188.28 and ΣHREE varies from 16.90 to 31.6. (La/Lu)N = 4.93 - 7.88; Eu/Sm = 0.313 - 0.43 (Ce/Yb)N = 3.58 - 5.27 and (La/Yb)n = 3.77 - 6.01. For norite ΣREE is 61.71, ΣLREE is 50.35 and ΣHREE 11.36. (La/Lu)N = 7.88; Eu/Sm = 0.45 (Ce/Yb)N =3.42 and (La/Yb)n = 3.56.

For ultrabasic type ΣREE is 15.58, ΣLREE is 12.05 and ΣHREE is 3.53. (La/Lu) N = 2.78; Eu/Sm = 0.26, Ce/Yb)N = 2.37 and (La/Yb)n = 2.73. These are highly depleted in REE.

All these rocks show negative Eu anomaly **(Fig. 6.12A)** except one basic charnockite and norite where it is slightly +ve and one basic charnockite (MS-4 : Kanpura) where no anomaly is perceptible. Ultrabsic type (Kanpura)exhibitsa distinct Tb +ve anomaly. LREE enrichment is observed in all the samples more conspicuously in the acid and intermediate varieties. REE patterns are suggestive of moderate fractionation in acid and intermediate type and slightly lower fractionation in basic variety **(Fig. 6.12B)**.

There is a remarkable similarity in REE patterns of acid and intermediate type of the study area and those from Deogarh-Nashirabad (Gyani & Omar, 1996), Pallavaram (Weaver, 1980) and somewhat similar pattern is seen in acid charnockite (Upper Archaean) of Qianan province of China (Wang et al, 1985) **(Fig. 6.13A)**. These patterns are also similar to Archaean andesite, rhyolite and quartz-monzonite, indicative of igneous protolith. These are also similar to Lewisian intermediate granulite (Weaver and Tarney, 1980).

REE patterns of basic variety are comparable with Archaean andesites (Condie, 1976c, 1981a) in **Fig 6.13B**. LREE enrichment patterns are comparable to continental tholeiites or P-type MORB characters (Jahn, 1990). Lingadevaru et al. (1996) have also suggested that mafic granulites from Hanur show slightly enriched LREE & flat HREE patterns without any significant Eu anomaly and are characteristic of Archaean tholeiites and are comparable to Island Arc tholeiites.

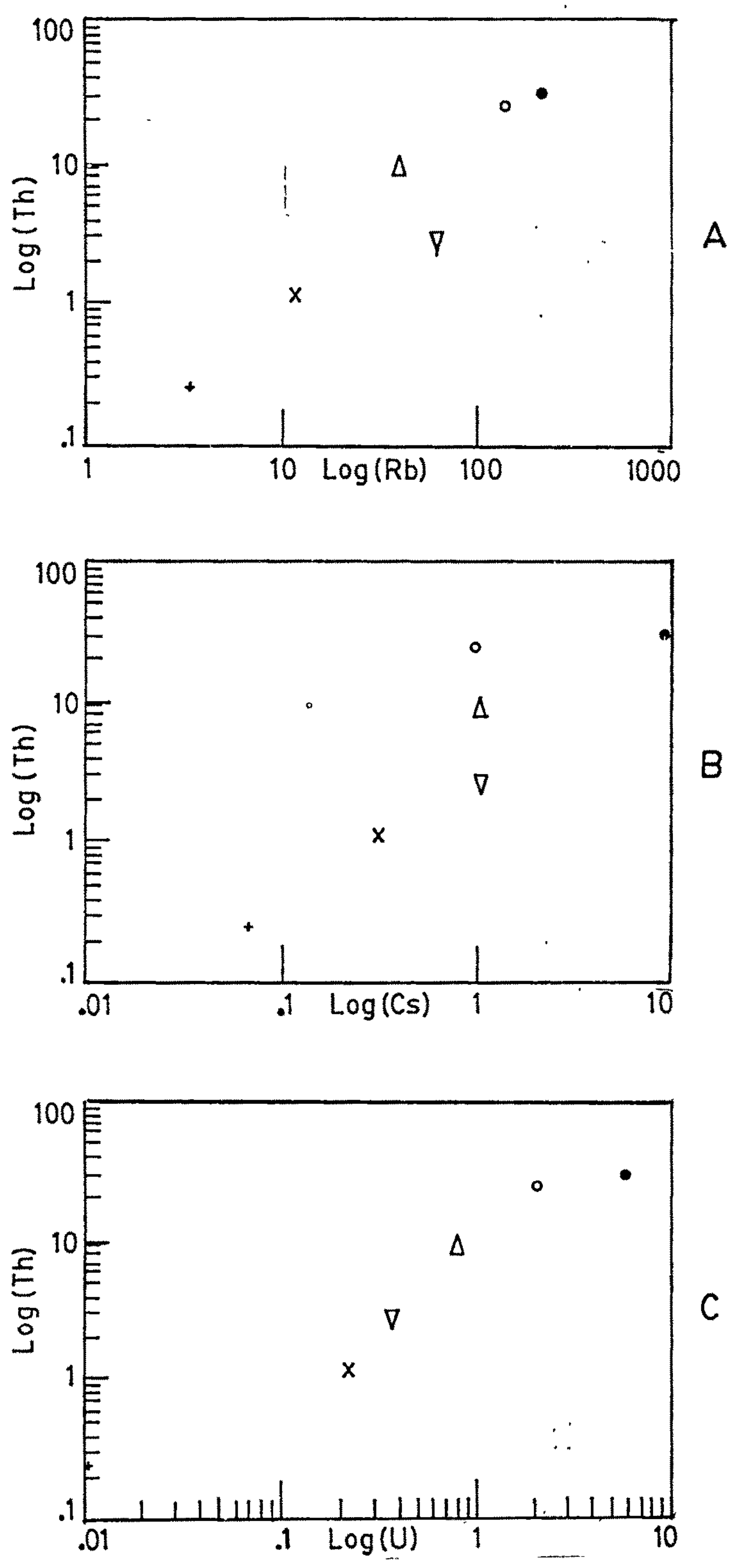

Fig. 6.11 **A, B, C Log Th vs Log Rb, Log Cs and Log U plots in 2-pyroxene granulites.**

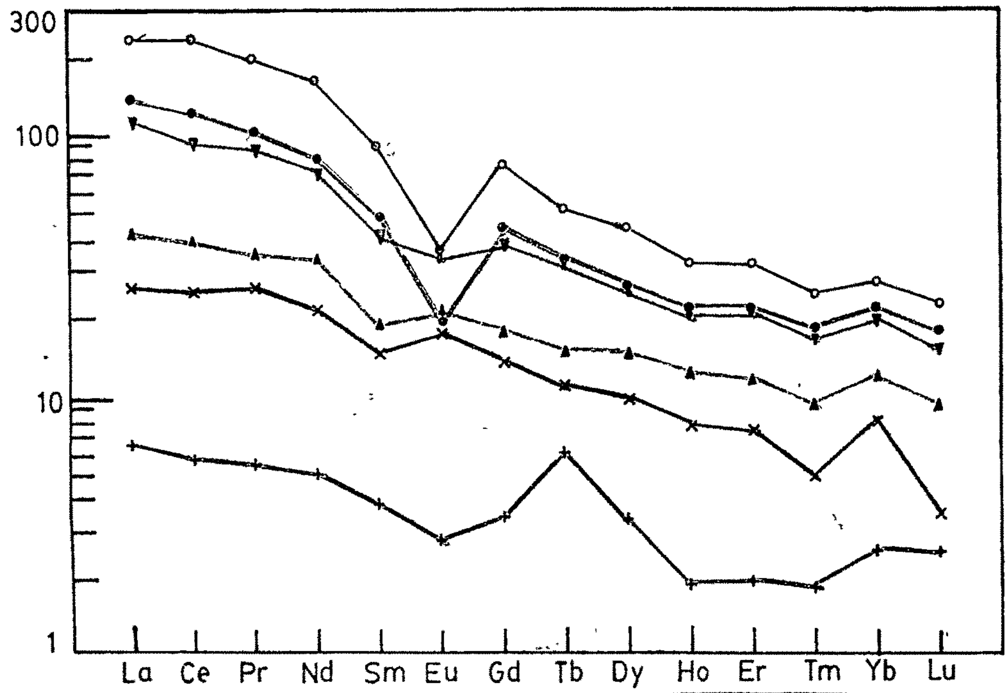

Fig. 6.12A REE pattern of 2-pyroxene granulites.

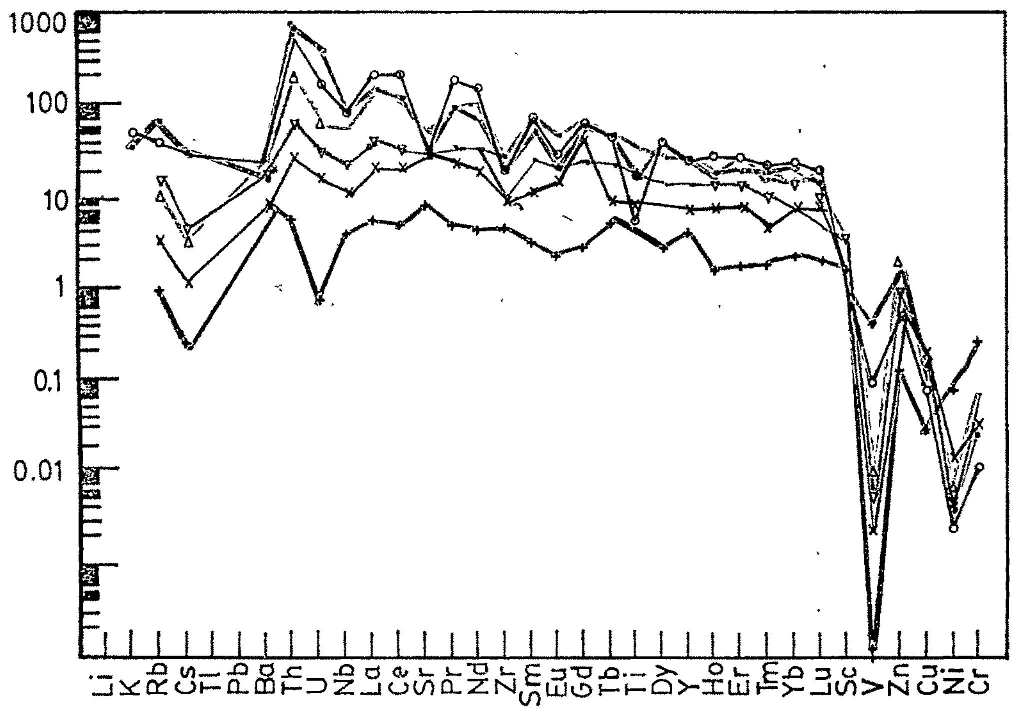

Fig. 6.12B Extended REE pattern of 2-pyroxene granulites.

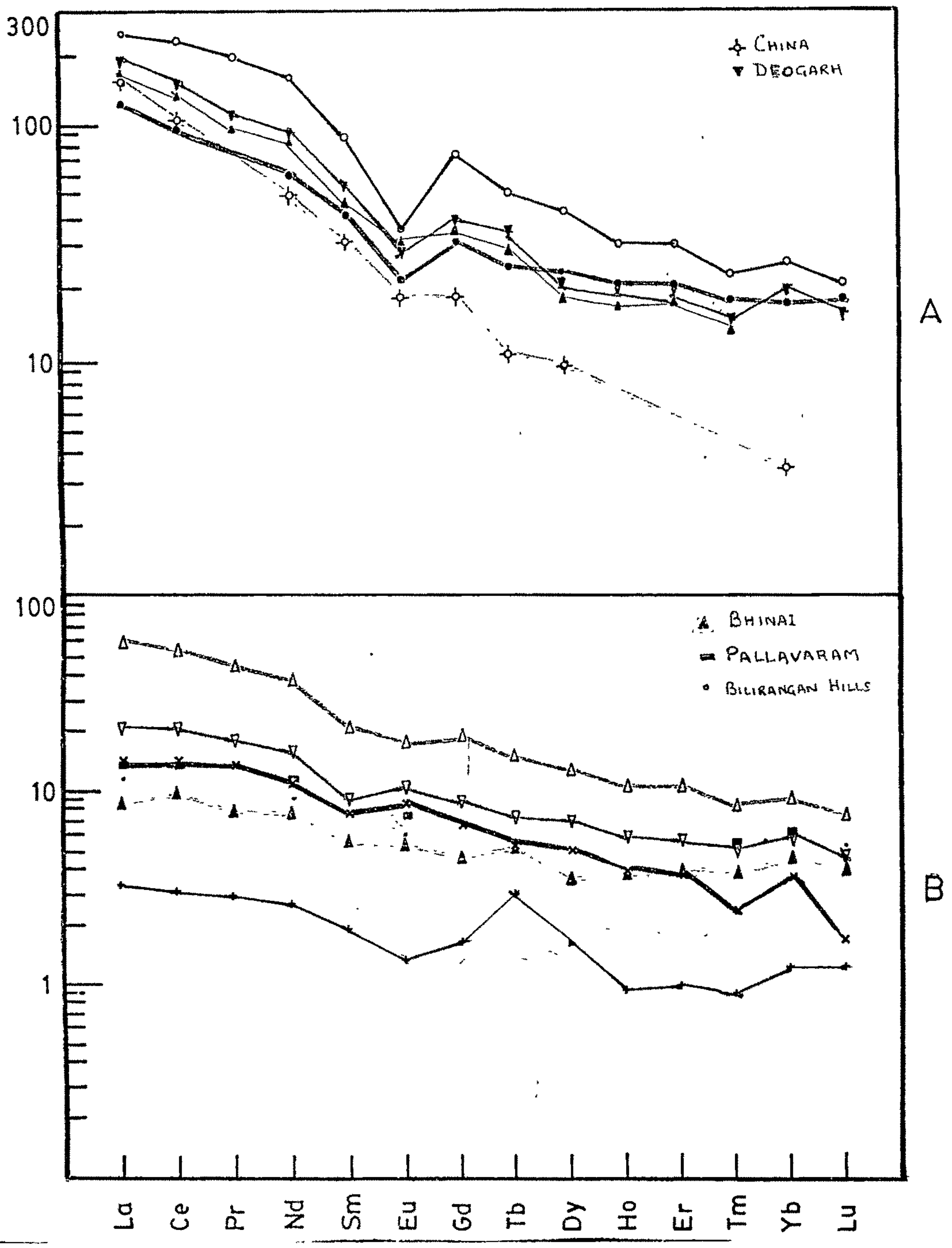

Fig. 6.13A Comparison of REE pattern of acid and intermediate granulites

Fig. 6.13B Comparison of REE patterns of basic and ultrabasic 2-pyroxene granulites.

REE patterns are also comparable with those of basic granulite of Pallavaram, Madras (Weaver, 1980) particularly MP-43 and those from Bhinai-Bandanwara sector (Gyani & Omar, 1996) of Rajasthan. Weaver (op cit) has inferred an extremely heterogenous source or a number of distinct sources for Madras granulites and charnockites evolving under extremely reducing conditions. He has attributed Eu -ve anomaly to low-pressure feldspar fractionation.

The present basic varieties represent low fractionated REE patterns with slight --ve Eu anomaly which may be due to feldspar fractionation during high grade metamorphism.

Thus from the major element behaviour of the rocks it is deduced that basic rocks of varied composition viz. anorthosite, gabbro and norite - continental tholeiites were the precursors of the basic and ultrabasic types.

From the chemical behaviour of all types of charnockites,it is suggested that their protoliths were all igneous rocks (tonalite / adamellite / quartz-monzonite / granodiorite-tholeiites), with the development of minerals exhibiting metamorphic transformations.

The trace element geochemistry of the rocks, which shows large variation in their abundances also suggests varied mineralogy of the precursors of the charnockitic rocks.

The different models of charnockite formation (after Jahn, 1990) are :

1. Charnockite represents H_2O under-saturated magma (dry melt) formed due to granulite facies metamorphism, i.e. in situ dry anatexis during granulite facies event.
2. Charnockites are residues (restite) after removal of granitic partial melt under high P-T conditions (Fyfe, 1973; Pride & Muecke, 1980; Powel, 1983; Clemens and Veilzeuf, 1987).
3. Charnockites may be taken as cumulates of igneous fractionation (cf. Field et al., 1980).
4. Charnockites are formed by granulite facies metamorphism involving high CO_2 activities (Newton et al., 1980; Newton, 1987; Janardhan et al. 1982).

In the light of geochemical evidences (and metamorphic evolution discussed later in Chapter-VII),all the above mentioned processes (particularly 1, 2 and 4) appear to have jointly contributed in the formation of charnockites. However, the production of acid and intermediate charnockites due to anatexis during granulite facies event should not be ruled out as anatexis also explains widespread migmatisation in pelitic granulites and scapolitisation of plagioclase due to migmatisation in calc granulites.

VI.3 PELITIC GRANULITES AND CALC GRANULITES

The different oxides of metapelites are plotted against SiO_2 in **Fig. 6.14** to show their variations. In general it is seen that in pelitic granulites :

(i) TiO_2 increases with increase in SiO_2;

(ii) Al_2O_3 and FeO* decrease with SiO_2

(iii) Na_2O and K_2O increase with SiO_2

(iv) MgO decreases with increase of SiO_2

Compositions of these granulites reveal their bimodal composition and have been plotted in terms of CaO-Na_2O-K_2O **(Fig. 6.15A)** and normative Ab-An-Or **(Fig. 6.15B)**. Pelitic granulites occupy the field of granodiorite, adamellite and granite. It can be inferred that rocks had both basic and acid igneous rocks as their precursors.

Normative Q-Ab-Or and ACF plots show higher quartz content than Archaean metasediments and more albite than Proterozoic gneisses and indicate paucity in Or content **(Fig.6.16A)**. As per Miyashiro's classification (1973, 1994), most of the plots are within the field of shales **(Fig. 6.16B)** & greywackes.

In the AFM diagram, most of the plots are seen to be within the field of Sargur Gneiss and some occupy the field of the well established Archaean Amitsoq Gneiss, in their chemical characters **(Fig. 6.17A)**.

In the (FeO + MgO)-Na_2O-K_2O diagram **(Fig. 6.17B)**, most of the metasediments plot in fields of sodic sandstone and ferromagnesian potassic sandstones.

In CaO-Na_2O-K_2O and FeO-MgO-(Na_2O-K_2O) plots most of protoliths of metasediments fall in/near the field of Dharwar geosynclinal sediments, few in Dharwar greenstone volcaniclastics and basalt fields **(Fig. 6.18 A & B)**. Most of these are outside the ~~field of orthoquartzite-carbonate~~ sediments of mid to late Proterozoic Cuddapah & Kurnools (S.India).

In the K_2O vs Na_2O and Rb (ppm) plots, it is seen that Na_2O increases with K_2O **(Fig.6.19 A & B)**; Rb is very high as compared to Khondalite of Pallavaram, Graywacke of Dharwars and Metapelites of Deogarh Nashirabad of Central Rajasthan (Gyani & Omar, 1996).

Rb/Sr ratio is about 3.49 (compared to Central Rajasthan : 0.43-2.92).

K/Rb ratio is 149.8 for the pelitic granulites of the study area (it is 226 - 369 for Deogarh Nashirabad pelitic granulites).

In the Th-Hf-Co and La-Th-Sc diagrams the pelitic granulites plot outside field of the post Archaean shales **(Figs. 6.20A and 6.20B)**.

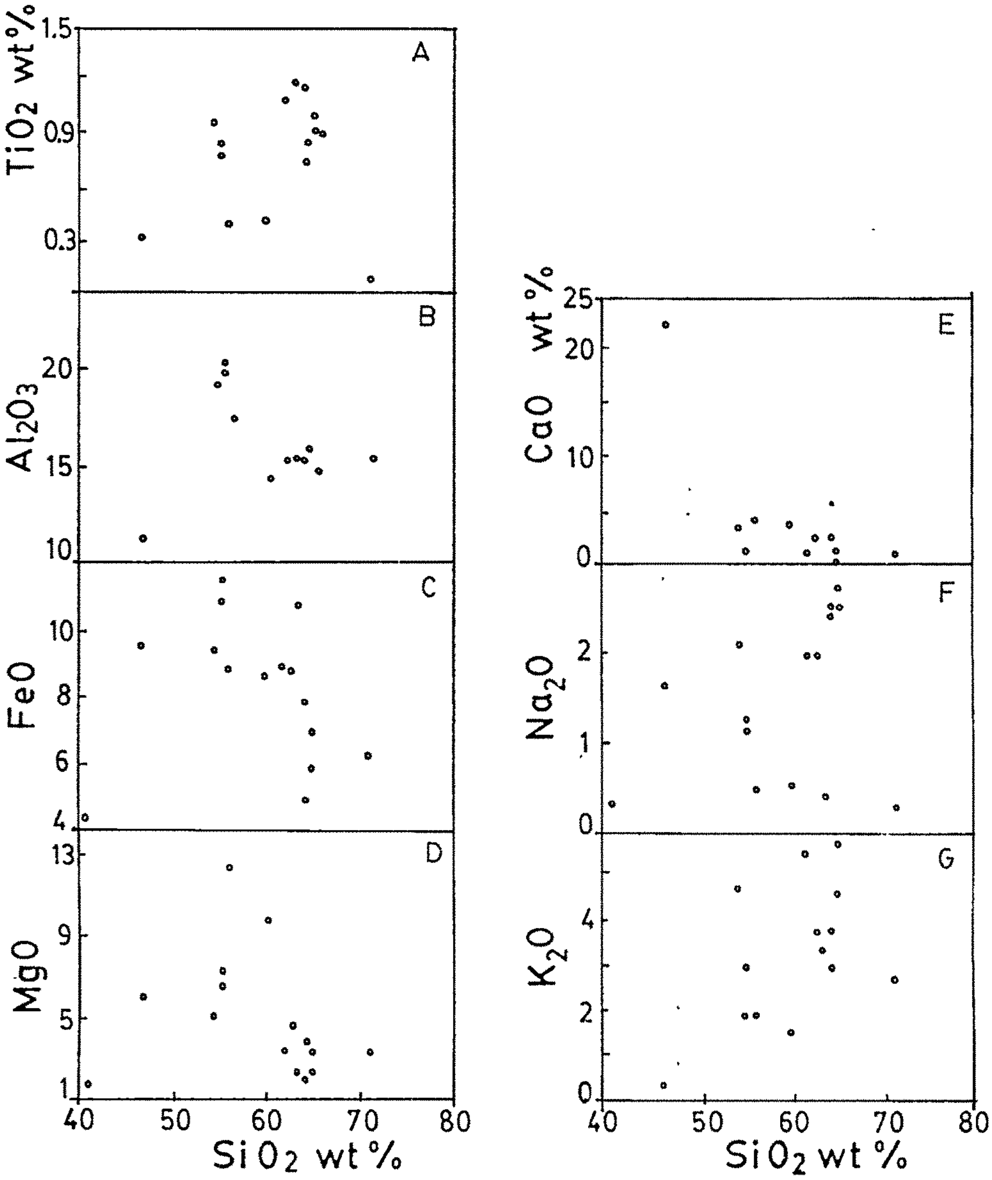

Fig. 6.14 Plots of SiO2 vs various oxides in metapelites.

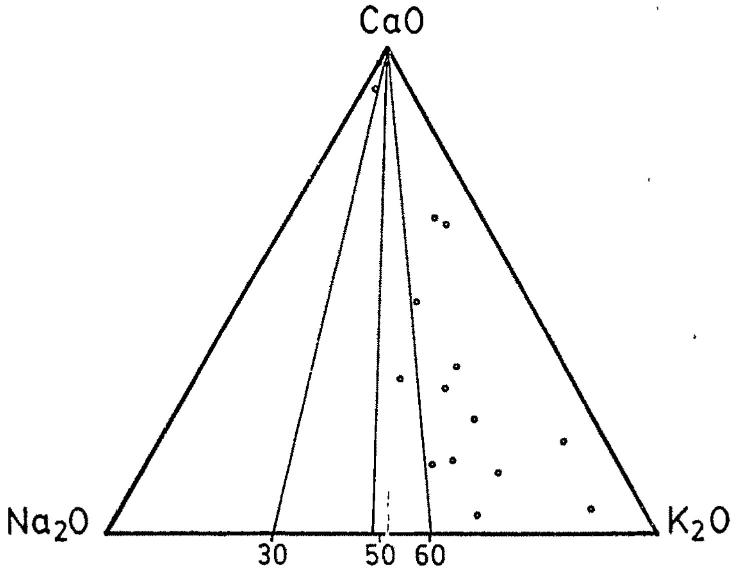

Fig. 6.15A CaO-Na2O-K2O diagram of pelitic granulites

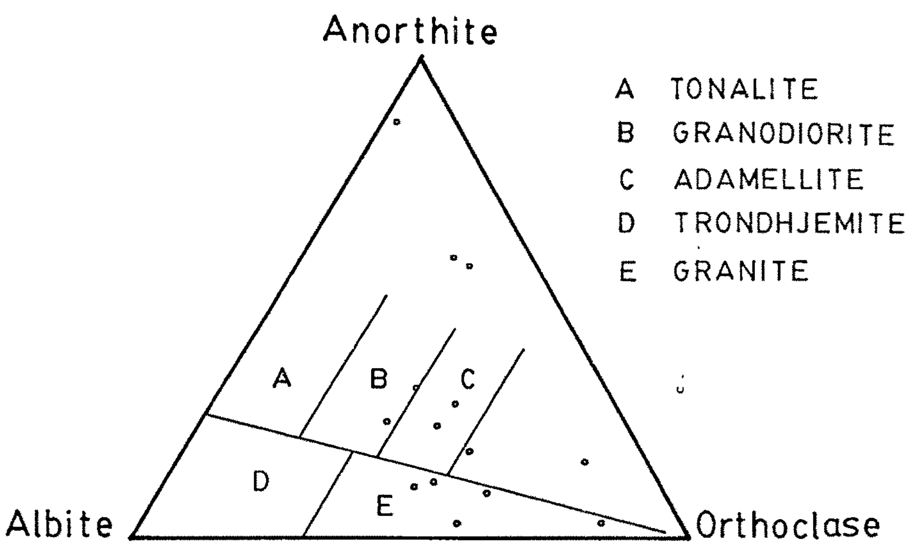

Fig. 6.15B Normative Ab-An-Or diagram of Pelitic granulites

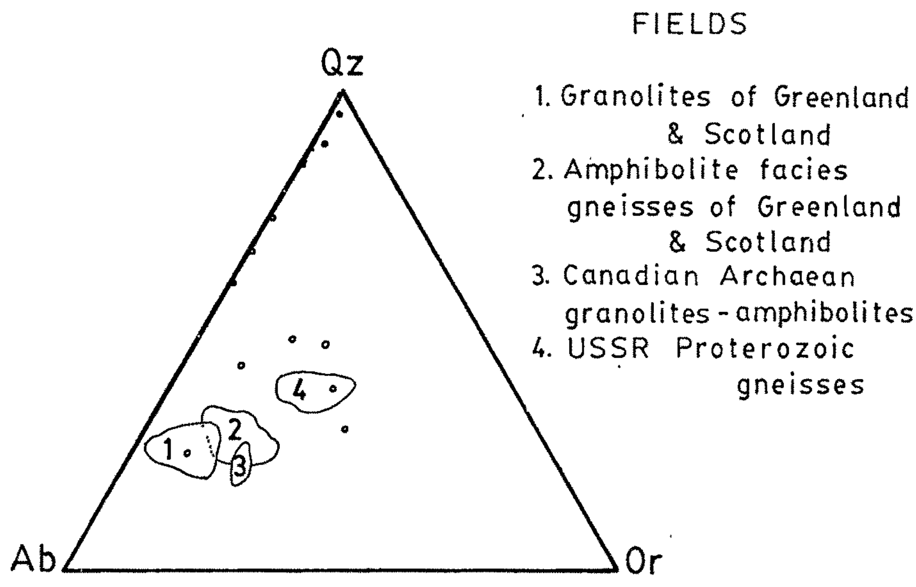

Fig. 6.16A Normative Qz-Ab-Or diagram of pelitic granulites.

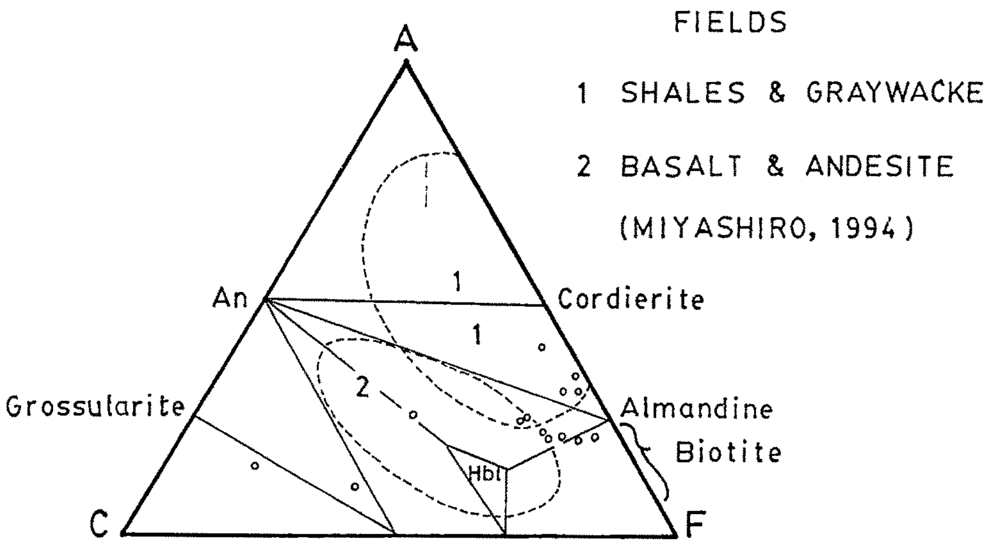

Fig. 6.16B ACF plots of pelitic granulites (Miyashiro's classification (1973, 1994).

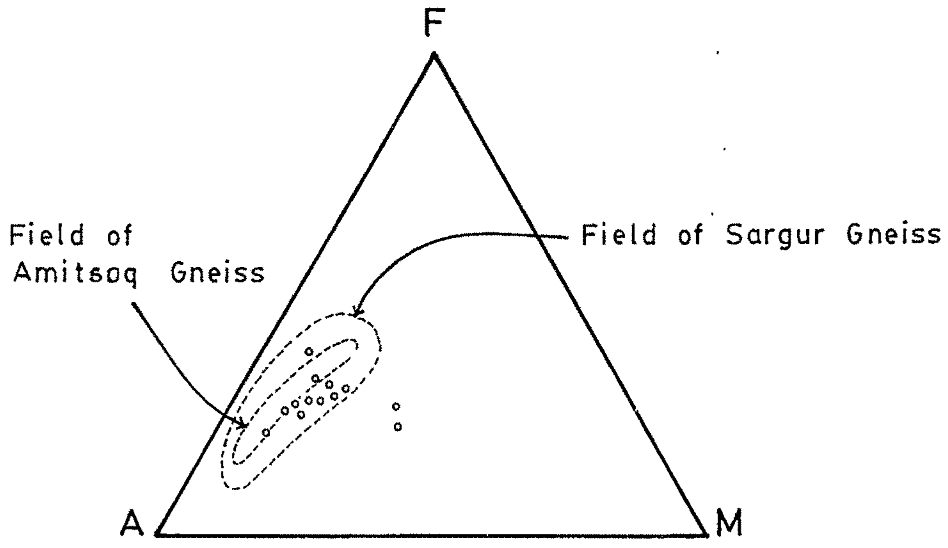

Fig. 6.17A AFM diagram of pelitic granulites.

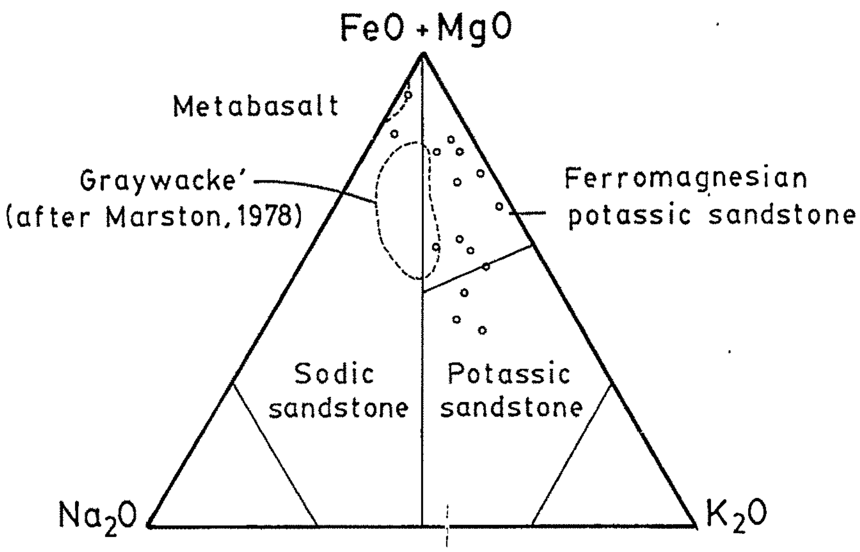

Fig. 6.17B (FeO + MgO)-Na2O-K2O diagram of the metasediments

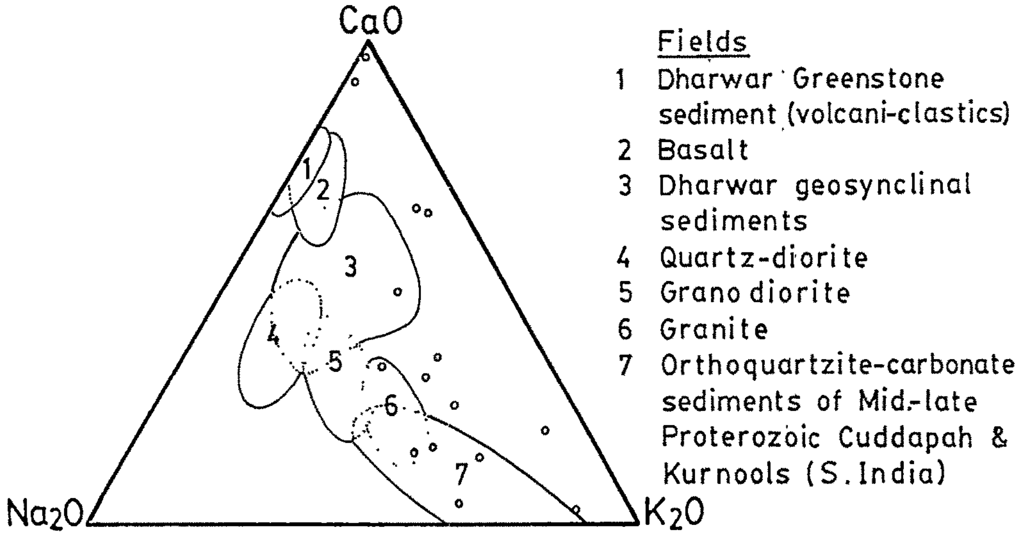

Fig. 6.18A CaO-Na2O-K2O diagram of metasediments

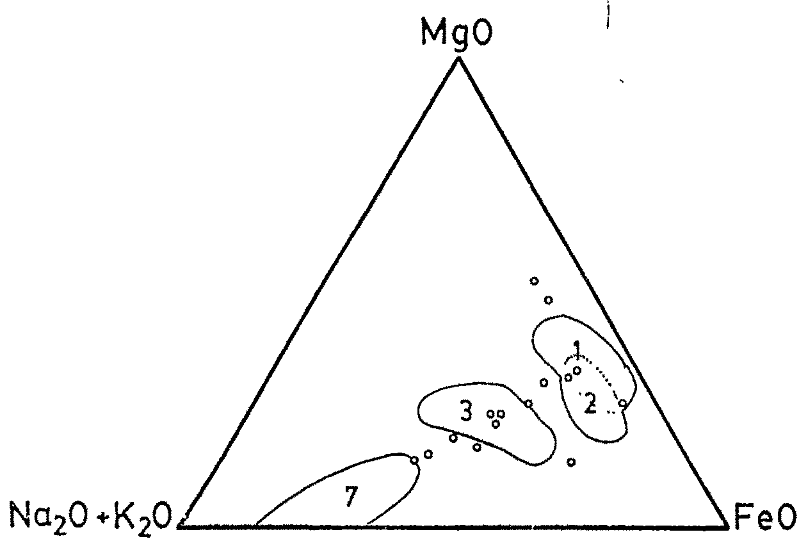

Fig. 6.18B FeO-MgO-(Na2O+K2O) plots of metasediments.

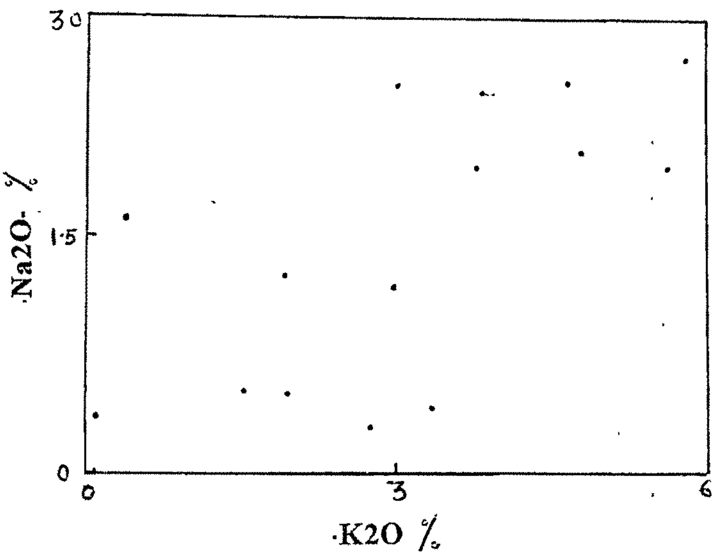

Fig. 6.19A K2O vs Na2O plots of pelitic granulites

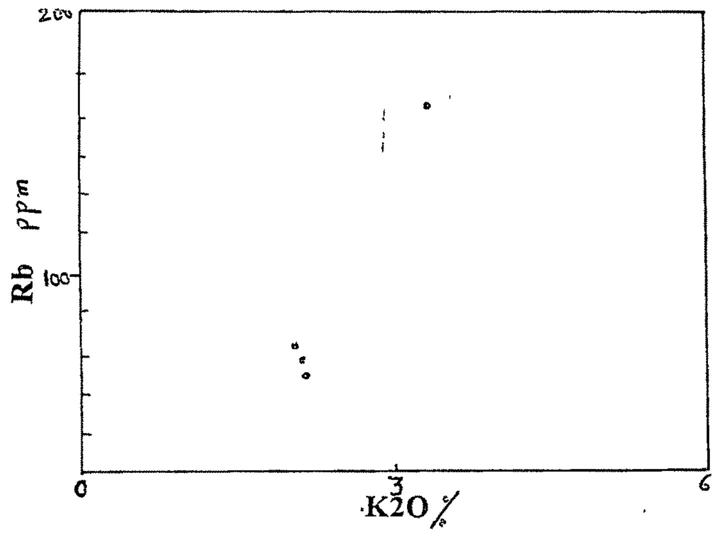

Fig. 6.19B K2O vs Rb (ppm) plots of pelitic granulites.

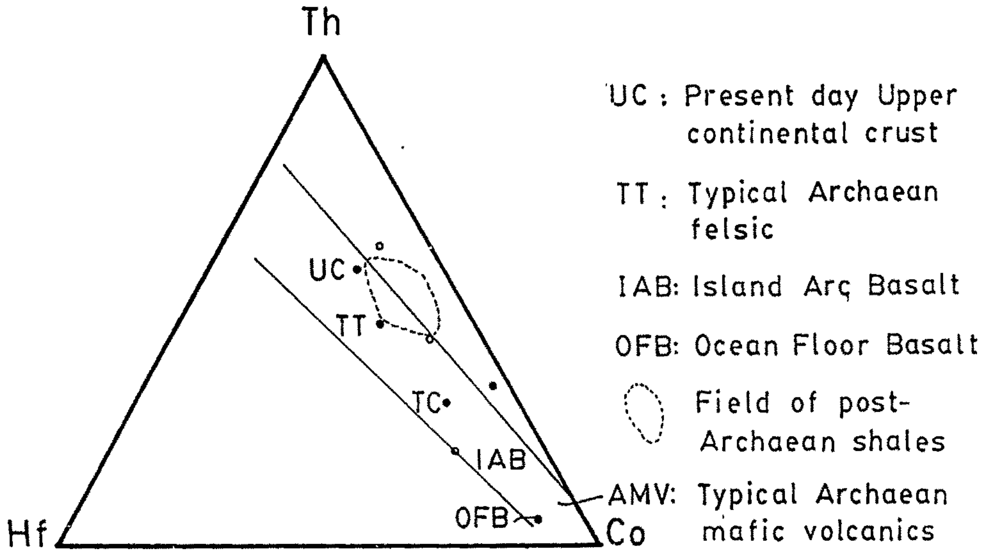

Fig. 6.20A Th-Hf-Co diagram of the pelitic granulites

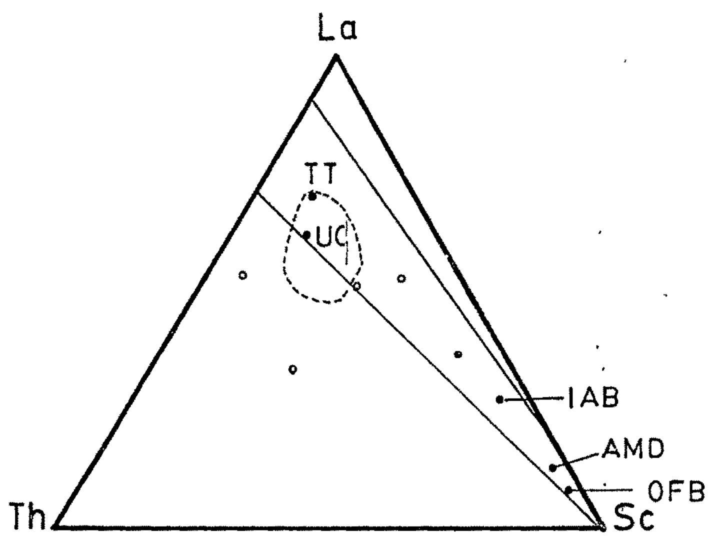

Fig. 6.20B La-Th-Sc diagram of the pelitic granulites

The metasediments of the area are plotted on a ratio-ratio plot of Co/Th vs La/Sc. The chemical plots correspond well to mixing curve (Mc Lennan and Taylor, 1984). The pelitic granulites plot close to those of Pilbara and S.Africa while the calc granulites plot close to Central Rajasthan, S. Africa and Pilbara **(Fig. 6.21A)** and support two component mixing model of the Archaean bimodal metasediments.

REE for pelitic and calc granulite of the study area have been compared in chondrite normalised plot in **Fig. 6.21B**. The REE patterns compare very well with those of Deogarh Nashirabad of C. Rajasthan (Gyani & Omar, 1996).

Total REE for pelitic granulites is 230.8. Total LREE is 207.80 and total HREE is 23.00.

Total REE for calc granulites is 96.61. Total LREE is 85.79 and total HREE is 10.82.

This indicates that either LREE are enriched or there is depletion of HREE.

Jakes and Taylor (1974) concluded that high Eu in the Precambrian sediments reflects abundances of igneous rocks in the source region. In that case the sediments of the region may have been derived from sources with high proportion of volcanics and plutonic rocks of acid/basic composition.

Typical REE patterns in the Archaean sedimentary rocks differ in three significant respects from those of post-Archaean sedimentary rocks :

(i) They have lower La/Yb ratio with average $(La/Yb)_N = 4.6$;

(ii) No significant Eu anomaly; and

(iii) Low Total REE =70 compared to 185 for post-Archaean average Australian Sedimentary rocks.

Thus it is evident that the metasediments of the study area with ∑REE 90-148 compare well with Archaean metasediments of the world and have basic and acid igneous rocks as their protoliths.

VI.4 For ***Erinpura granite*** ∑REE is 484.42, ∑LREE is 412.96 and ∑HREE is 71.46. (La/Lu)N = 5.73; Eu/Sm = 0.043, (Ce/Yb)N = 4.28 and (La/Yb)n = 5.22. The REE patterns for the Erinpura granite are distinctly different from the charnockite suite of rocks **(Fig. 6.22A)**. Eu -ve anomaly is very prominant. In Erinpura granites ∑REE is highest of all the samples (484.42). **(Fig. 6.22B)**. This also indicates that Erinpura granite could not be responsible for giving rise to intermediate and acid charnockites which predate the emplacement of Erinpura granite. However the regional metamorphism and associated migmatisation (M3) that synchronised with and outlasted Delhi deformation (D3) as also the thermal imprints visualised by Desai et al (op cit) should be related to Erinpura granite event.

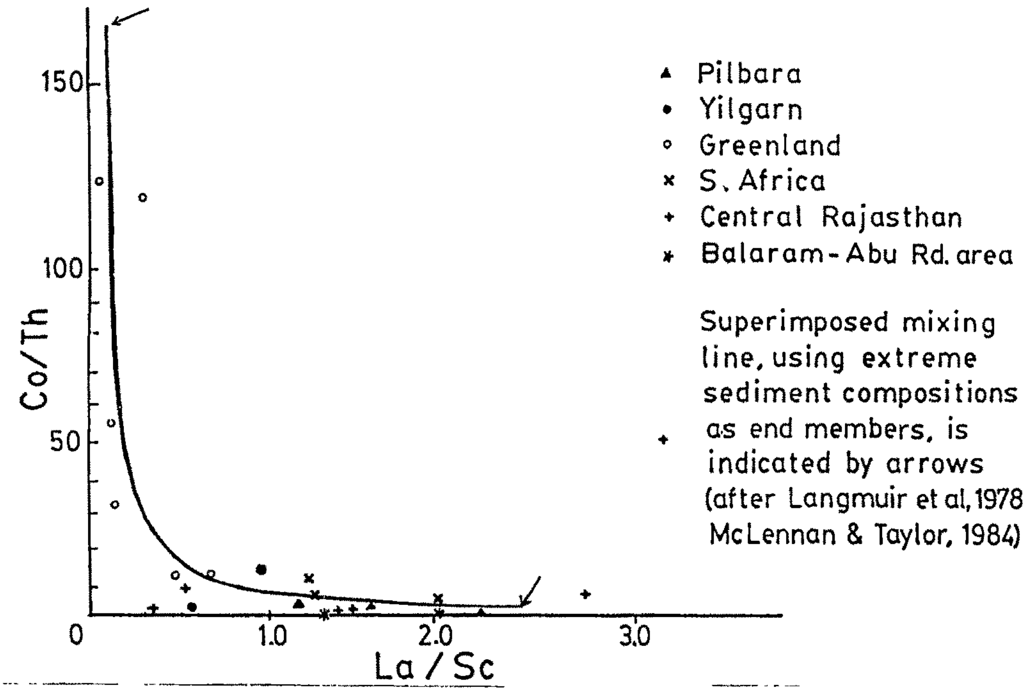

Fig. 6.21A Ratio-ratio plot of Co/Th vs La/Sc in pelitic granulites.

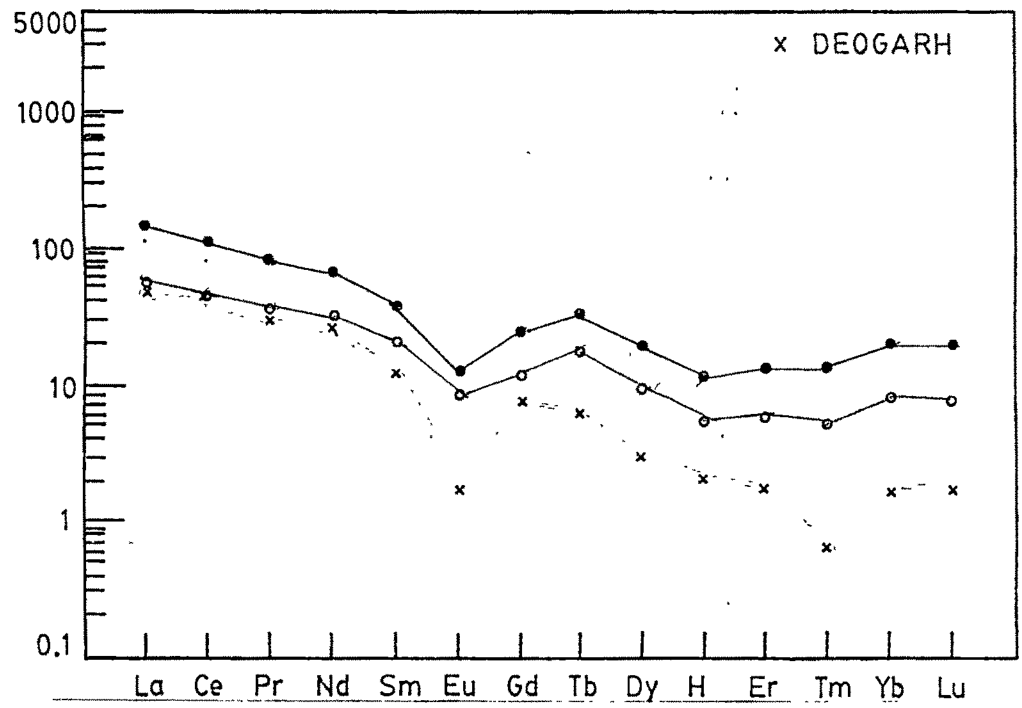

Fig. 6.21B Chondrite normalised REE plots showing comparison between pelitic and calc granulites of the study area and those of Deogarh Nashirabad of C. Rajasthan.

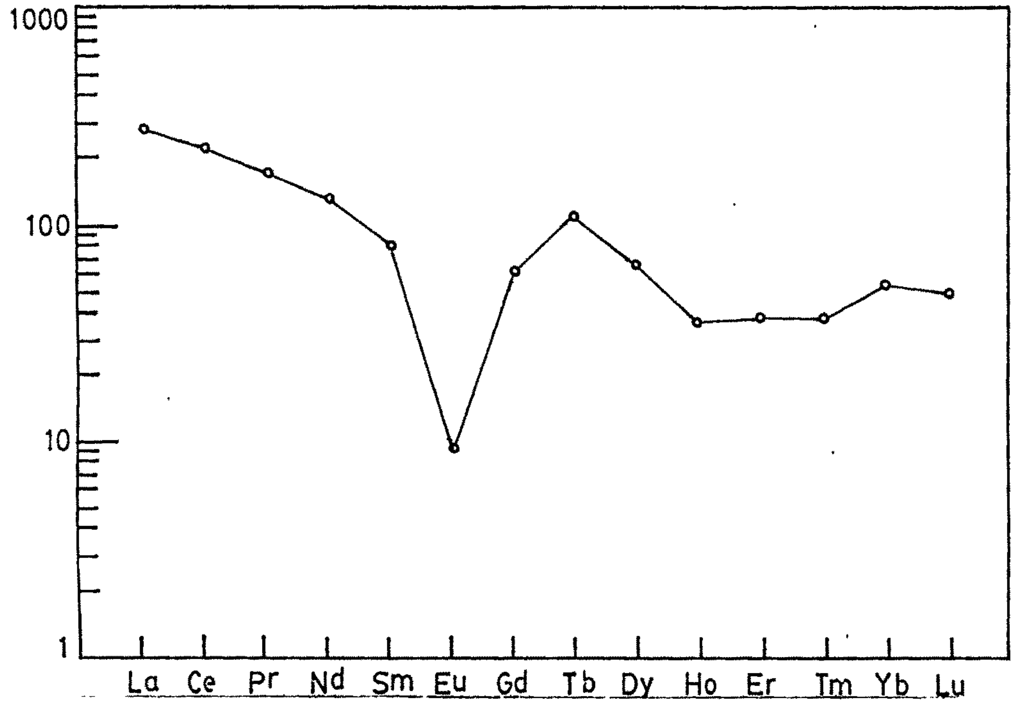

Fig. 6.22A REE pattern of Erinpura Granite

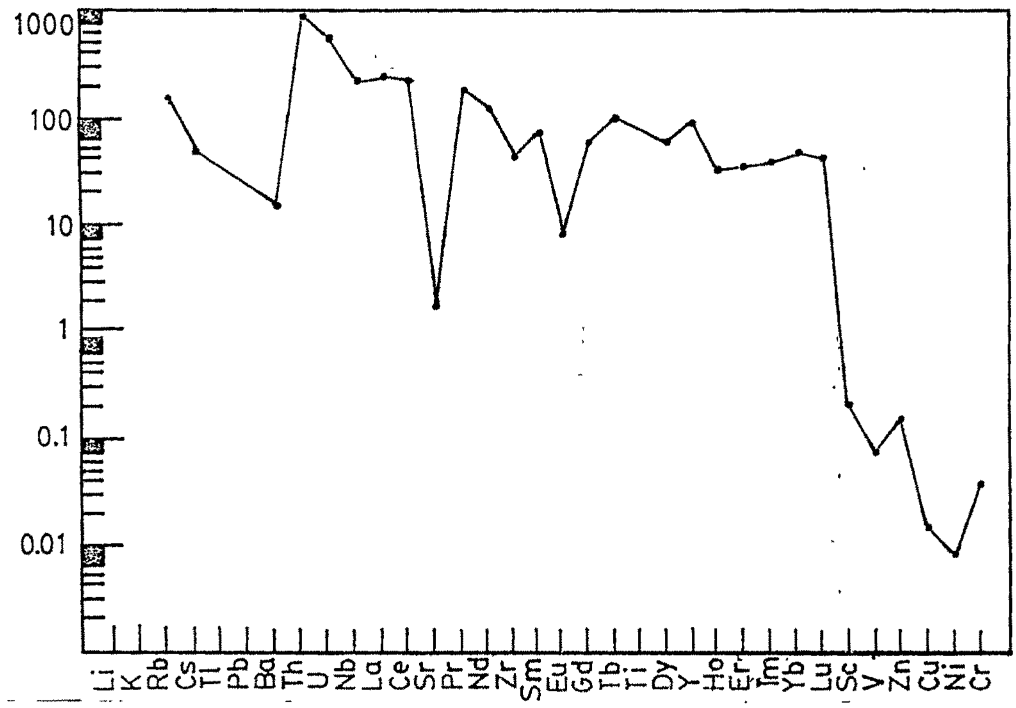

Fig. 6.22B Extended REE pattern of Erinpura Granite

TABLE-VI.1

Major oxide analyses of 2-pyroxene granulites

Sample:	SJDMPP-1		SJDMPP-2		SJDMPP-3		SJDMPP-4		SJDMPP-5	
Oxide	WT %	Mole%	WT %	Mole%	WT %	Mole%	WT %	Mole%	WT %	Mole%
SiO_2	46.70	46.63	47.54	45.83	47.85	49.94	48.97	49.87	47.05	49.31
TiO_2	0.57	0.43	1.09	0.79	0.64	0.50	0.71	0.54	0.98	0.77
Al_2O_3	9.20	5.41	6.35	3.61	13.64	8.39	12.07	7.24	12.82	7.92
Fe_2O_3	0.00	0.00	0.00	0.00	0.00	0.00	0.00	0.00	0.00	0.00
FeO	15.79	13.19	15.88	12.81	15.06	13.15	11.75	10.01	15.97	14.00
MnO	0.21	0.18	0.13	0.11	0.18	0.16	0.15	0.13	0.22	0.20
MgO	15.21	22.64	18.98	27.27	8.47	13.18	10.45	15.86	8.24	12.87
CaO	9.84	10.53	8.70	8.99	10.44	11.68	12.38	13.51	10.84	12.18
Na_2O	0.93	0.90	0.48	0.45	2.71	2.74	2.49	2.46	2.01	2.04
K_2O	0.04	0.03	0.11	0.07	0.26	0.17	0.34	0.22	0.91	0.61
P_2O_5	0.15	0.06	0.21	0.09	0.21	0.09	0.38	0.16	0.23	0.10
Total	98.64	100.00	99.47	100.02	99.46	100.00	99.69	100.00	99.27	100.00

Sample:	SJDMPP-6		SJDMPP-7		SJDMPP-8		SJDMPP-9	
Oxide	WT %	Mole%	WT %	Mole%	WT %	Mole%	WT %	Mole%
SiO_2	60.81	67.09	61.85	66.66	67.16	73.25	71.94	78.26
TiO_2	1.01	0.84	0.83	0.67	0.16	0.13	0.41	0.34
Al_2O_3	14.85	9.66	13.97	8.87	16.99	10.92	13.20	8.46
Fe_2O_3	0.00	0.00	0.00	0.00	0.00	0.00	0.00	0.00
FeO	9.66	8.92	8.31	7.49	3.37	3.07	3.39	3.08
MnO	0.15	0.14	0.05	0.05	0.01	0.01	0.03	0.03
MgO	1.27	2.09	2.56	4.11	0.95	1.54	0.68	1.10
CaO	4.37	5.17	5.71	6.59	3.51	4.10	2.18	2.54
Na_2O	4.05	4.33	3.78	3.95	4.45	4.71	2.89	3.05
K_2O	2.45	1.72	2.01	1.38	3.04	2.12	4.34	3.01
P_2O_5	0.11	0.05	0.48	0.22	0.31	0.14	0.28	0.13
Total	98.73	100.01	99.55	99.99	99.95	99.99	99.34	100.00

CIPW Norm

Sample:	SJDMPP-	1	2	3	4	5	6	7	8	9
	Mineral	WT %	WT %	WT %	WT %	WT %	WT %	WT %	WT %	WT %
Q	Quartz	0.00	0.00	0.00	0.00	0.00	10.74	13.26	18.87	31.07
C	Corundum	0.00	0.00	0.00	0.00	0.00	0.00	0.00	0.74	0.46
Or	Orthoclase	0.24	0.65	1.54	2.01	5.38	14.48	11.88	17.97	25.65
Ab	Albite	7.87	4.06	22.25	19.65	16.75	34.27	31.98	37.65	24.45
An	Anorthite	20.81	14.85	24.29	20.76	23.27	15.11	15.22	15.39	8.99
Ne	Nepheline	0.00	0.00	0.37	0.77	0.14	0.00	0.00	0.00	0.00
Di	Diopside	22.15	21.91	21.80	31.35	24.25	5.08	8.47	0.00	0.00
Hy	Hypersthene	20.76	32.07	0.00	0.00	0.00	16.88	16.05	8.30	7.30
Ol	Olivine	25.38	23.37	27.51	22.92	27.08	0.00	0.00	0.00	0.00
Il	Ilmenite	1.08	2.07	1.22	1.35	1.86	1.92	1.58	0.30	0.78
Ap	Apatite	0.36	0.50	0.50	0.90	0.54	0.26	1.14	0.73	0.66
	Total	98.65	99.49	99.47	99.71	99.28	98.74	99.57	99.96	99.35

Sample :	SJMPP-	1	2	3	4	5	6	7	8	9
	Formula	Mole%	Mole%	Mole%	Mole%	Mole%	Mole%	Mole%	Mole%	Mole%
Q	SiO_2	0.00	0.00	0.00	0.00	0.00	34.56	39.74	50.45	66.69
C	Al_2O_3	0.00	0.00	0.00	0.00	0.00	0.00	0.00	1.17	0.58
Or	$(K,Na)AlSi_3O_8$	0.19	0.49	1.25	1.61	4.37	10.06	7.69	10.37	11.89
Ab	$(K,Na)AlSi_3O_8$	6.54	3.27	19.13	16.68	14.45	25.27	21.96	23.06	12.03
An	$(Na,K)AlSi_2O_8$	16.32	11.25	19.69	16.60	18.93	10.50	9.85	8.89	4.17
Ne	$(Na,K)(Al,Si)_2O_4$	0.00	0.00	0.59	1.20	0.22	0.00	0.00	0.00	0.00
Di	$Ca(Mg,Fe)(SiO_2)_3$	21.19	20.42	21.19	30.54	23.58	4.07	6.46	0.00	0.00
Hy	$(Mg,Fe)SiO_3$	20.24	30.71	0.00	0.00	0.00	13.00	12.03	5.51	3.83
Ol	$(Mg,Fe)_2SiO_4$	33.82	30.78	36.12	31.01	35.43	0.00	0.00	0.00	0.00
Il	$FeTiO_3$	1.56	2.88	1.81	1.98	2.77	2.44	1.87	0.32	0.66
Ap	$Ca_5(PO_4)_3F$	0.15	0.21	0.22	0.40	0.24	0.10	0.41	0.23	0.17
Total		100.00	100.00	100.00	100.00	100.00	100.00	100.00	100.00	100.00

TABLE-VI.2

Major oxide analyses (by XRF)

Oxide	MS-2 WT %	MS-2 Mole%	MS-4 WT %	MS-4 Mole%	MS-1 WT %	MS-1 Mole%	MS-7 WT %	MS-7 Mole%	MS-10 WT %	MS-10 Mole%
SiO_2	64.70	72.09	52.40	60.14	69.75	76.91	63.50	71.47	40.82	50.49
TiO_2	1.23	1.03	2.14	1.85	0.55	0.46	1.16	0.98	0.46	0.43
Al_2O_3	12.32	8.09	13.97	9.45	13.06	8.49	15.36	10.19	10.09	7.36
Fe_2O_3	0.00	0.00	0.00	0.00	0.00	0.00	0.00	0.00	0.00	0.00
FeO	5.93	5.53	9.73	9.34	4.11	3.79	10.71	10.08	4.36	4.51
MnO	0.09	0.08	0.16	0.16	0.08	0.07	0.18	0.17	0.08	0.08
MgO	1.76	2.92	2.86	4.89	0.31	0.51	2.33	3.91	1.80	3.32
CaO	3.85	4.60	7.78	9.57	1.98	2.34	0.21	0.25	24.91	33.02
Na_2O	2.73	2.95	2.64	2.94	3.54	3.78	0.39	0.43	0.36	0.43
K_2O	3.61	2.57	1.87	1.37	5.07	3.57	3.34	2.40	0.08	0.06
P_2O_5	0.23	0.11	0.49	0.24	0.12	0.06	0.05	0.02	0.12	0.06
Cr_2O_3	0.01	0.00	0.02	0.01	0.01	0.00	0.05	0.02	0.02	0.01
Total	98.46	99.97	96.06	99.96	98.58	99.98	97.28	99.92	83.10	99.77

CIPW Norm

	Mineral	MS-2 WT %	MS-4 WT %	MS-1 WT %	MS-7 WT %	MS-10 WT
Q	Quartz	22.10	6.79	23.17	36.33	0.12
C	Corundum	0.00	0.00	0.00	10.80	0.00
Z	Zircon	0.01	0.02	0.02	0.01	0.03
Or	Orthoclase	21.42	11.07	30.02	19.81	0.47
Ab	Albite	23.10	22.34	29.95	3.30	3.05
An	Anorthite	10.68	20.75	4.76	0.82	25.71
Di	Diopside	5.93	12.52	3.79	0.00	23.65
Wo	Wollastonite	0.00	0.00	0.00	0.00	29.21
Hy	Hypersthene	10.41	15.42	5.58	23.93	0.00
Cm	Chromite	0.01	0.02	0.01	0.07	0.03
Il	Ilmenite	2.34	4.06	1.04	2.20	0.87
Ap	Apatite	0.55	1.16	0.28	0.13	0.29
Total		96.53	94.15	98.63	97.40	83.42

	Formula	MS-2 Mole%	MS-4 Mole%	MS-1 Mole%	MS-7 Mole%	MS-10 Mole%
Q	SiO_2	56.04	24.61	57.58	66.45	0.58
C	Al_2O_3	0.00	0.00	0.00	11.64	0.00
Z	$ZrSiO_4$	0.01	0.02	0.02	0.01	0.05
Or	$(K,Na)AlSi_3O_8$	11.72	8.66	16.10	7.82	0.50
Ab	$(K,Na)AlSi_3O_8$	13.42	18.54	17.05	1.38	3.41
An	$(Na,K)AlSi_2O_8$	5.84	16.23	2.55	0.32	27.11
Di	$Ca(Mg,Fe)(SiO_2)_3$	3.83	11.55	2.32	0.00	29.63
Wo	$CaSiO_3$	0.00	0.00	0.00	0.00	36.83
Hy	$(Mg,Fe)SiO_3$	6.63	14.03	3.26	10.73	0.00
Cm	Cr_2O_4	0.01	0.02	0.01	0.04	0.04
Il	$FeTiO_3$	2.35	5.83	1.03	1.60	1.69
Ap	$Ca_5(PO_4)_3F$	0.16	0.50	0.08	0.03	0.17
Total		100.00	100.00	100.00	100.00	100.00

Table-VI.3 CHEMICAL ANALYSIS OF PELITIC AND CALC-GRANULITES

Sample	SJMP10	SJMP11	SJMP12	SJMP13	SJMP14	SJMP15	SJMP16	SJMP17	SJMP18	SJMP19
SiO_2	60.00	56.20	55.28	64.41	64.41	62.90	54.36	65.01	65.01	61.90
TiO_2	0.41	0.39	0.79	0.82	0.72	1.16	0.94	0.89	0.98	1.08
Al_2O_3	14.38	17.49	20.18	15.94	15.81	15.40	19.18	14.68	14.70	15.40
FeO*	8.66	8.82	10.89	7.88	4.82	8.75	9.41	6.89	5.83	8.97
MgO	9.68	12.18	6.49	3.78	1.94	4.48	5.04	3.25	2.25	3.38
CaO	3.84	4.32	1.30	2.60	5.78	2.48	3.64	1.37	0.37	1.18
Na_2O	0.52	0.49	1.20	2.54	2.50	1.98	2.10	2.57	2.75	1.98
K_2O	1.51	1.94	2.98	2.98	3.80	3.76	4.78	4.64	5.78	5.62
Total	99.00	101.83	99.11	100.95	99.78	100.91	99.45	99.30	97.67	99.51
Mg #	66.58	71.11	51.51	46.09	41.76	47.71	48.85	45.66	40.77	40.16
Density	2.58	2.62	2.59	2.49	2.45	2.51	2.56	2.46	2.42	2.49

Table-VI.4 RARE EARTH ELEMENTS AND TRACE ELEMENTS OF GRANULITES

Sample	MS-2	MS-4	MS-7	MS-10	MS-1	MS-3	MS-5	MS-6	MS-8	MS-9
Cr	35	110	340	126	41	174	134	1109	284	145
Ni	34	99	335	124	38	84	236	1260	271	134
Co	15	36	38	21	4	37	48	159	12	2
Sc	13	24	25	13	3	28	13	13	4	2
V	35	1	2	5	8	0	0	0	2	6
Cu	25	35	7	3	12	39	37	5	3	2
Zn	406	864	92	79	268	281	220	56	34	73
K	29968	15523	27726	664	42088	-	-	-	-	-
Rb	213	39	185	4	137	60	11	4	229	473
Cs	8.89	1.02	3.03	1.83	0.93	1.02	0.31	0.07	2.26	13.20
Ba	52	82	343	98	49	46	26	28	301	51
Sr	146	286	53	2237	75	278	395	90	64	22
Ga	22	20	34	20	25	18	16	7	18	37
Ta	1.96	1.37	1.08	3.36	2.74	0.65	0.35	0.14	0.87	4.80
Nb	20.2	16.1	20.4	11.0	35.0	8.0	4.4	1.6	18.0	77.8
Hf	1.72	3.30	1.54	4.29	3.27	0.92	1.48	0.47	3.75	9.39
Zr	57	85	63	155	98	27	53	25	122	232
Ti	7374	12829	6954	2758	3297	-	-	-	-	-
Y	55	43	53	20	53	27	18	10	28	183
Th	30.31	9.15	19.24	19.59	24.92	2.69	1.17	0.26	24.70	38.72
U	5.58	0.79	2.24	5.20	1.99	0.36	0.22	0.01	2.29	6.44
La	46.63	36.70	47.73	15.99	81.82	13.87	8.40	2.16	31.84	91.26
Ce	107.55	84.57	100.13	40.04	197.49	34.63	21.26	4.95	70.47	196.73
Pr	13.84	11.33	10.87	5.02	25.60	4.56	3.37	0.72	7.99	22.95
Nd	51.37	44.65	40.50	20.13	100.50	20.61	13.14	3.24	29.69	84.67
Sm	10.04	8.40	7.66	3.98	17.52	3.60	2.88	0.78	5.05	16.63
Eu	1.44	2.63	0.91	0.63	2.84	1.54	1.30	0.20	0.63	0.72
Gd	11.86	10.35	6.22	3.09	20.35	4.88	3.63	0.90	5.07	17.43
Tb	1.62	1.50	1.54	0.87	2.58	0.71	0.53	0.29	1.33	5.38
Dy	8.97	8.44	6.45	3.17	14.53	4.87	3.19	1.10	4.58	22.57
Ho	1.62	1.56	0.82	0.38	2.38	0.91	0.57	0.14	0.41	2.72
Er	4.74	4.65	2.84	1.23	6.81	2.47	1.59	0.43	1.14	8.73
Tm	0.59	0.54	0.43	0.17	0.81	0.31	0.16	0.06	0.15	1.31
Yb	4.50	4.08	4.10	1.67	5.79	2.46	1.58	0.53	1.18	11.68
Lu	0.59	0.48	0.60	0.24	0.72	0.29	0.11	0.08	0.16	1.64
Density	2.45	2.61	2.52	2.71	2.38	0.00	0.00	0.00	0.00	0.00

Table-VI.5 RARE EARTH ELEMENTS INTERPRETATION

SAMPLE	ΣREE	ΣLREE	ΣHREE	(La/Yb)N	(Ce/Yb)N	(La/Lu)N	Eu/Sm
MS-2	256.36	230.87	34.49	6.93	6.08	8.15	0.143
MS-4	219.88	188.28	31.60	6.01	5.27	7.88	0.313
MS-7	230.80	207.80	23.00	7.78	6.21	8.19	0.119
MS-10	96.61	85.79	10.82	6.39	6.09	6.86	0.158
MS-1	479.74	425.77	53.97	9.45	8.67	11.71	0.162
MS-3	94.17	77.27	16.90	3.77	3.58	4.93	0.430
MS-5	61.71	50.35	11.36	3.56	3.42	7.88	0.450
MS-6	15.58	12.05	3.53	2.73	2.37	2.78	0.260
MS-8	159.69	145.67	14.02	18.06	15.20	20.50	0.125
MS-9*	484.42	412.96	71.46	5.22	4.28	5.73	0.043

* ERINPURA GRANITES